



2016

# UTILIZATION OF A SMALL UNMANNED AIRCRAFT SYSTEM FOR DIRECT SAMPLING OF NITROGEN OXIDES PRODUCED BY FULL-SCALE SURFACE MINE BLASTING

Robert B. McCray

University of Kentucky, [rbmccr@gmail.com](mailto:rbmccr@gmail.com)

Digital Object Identifier: <http://dx.doi.org/10.13023/ETD.2016.330>

[Click here to let us know how access to this document benefits you.](#)

---

## Recommended Citation

McCray, Robert B., "UTILIZATION OF A SMALL UNMANNED AIRCRAFT SYSTEM FOR DIRECT SAMPLING OF NITROGEN OXIDES PRODUCED BY FULL-SCALE SURFACE MINE BLASTING" (2016). *Theses and Dissertations--Mining Engineering*. 31.

[https://uknowledge.uky.edu/mng\\_etds/31](https://uknowledge.uky.edu/mng_etds/31)

This Master's Thesis is brought to you for free and open access by the Mining Engineering at UKnowledge. It has been accepted for inclusion in Theses and Dissertations--Mining Engineering by an authorized administrator of UKnowledge. For more information, please contact [UKnowledge@lsv.uky.edu](mailto:UKnowledge@lsv.uky.edu).

**STUDENT AGREEMENT:**

I represent that my thesis or dissertation and abstract are my original work. Proper attribution has been given to all outside sources. I understand that I am solely responsible for obtaining any needed copyright permissions. I have obtained needed written permission statement(s) from the owner(s) of each third-party copyrighted matter to be included in my work, allowing electronic distribution (if such use is not permitted by the fair use doctrine) which will be submitted to UKnowledge as Additional File.

I hereby grant to The University of Kentucky and its agents the irrevocable, non-exclusive, and royalty-free license to archive and make accessible my work in whole or in part in all forms of media, now or hereafter known. I agree that the document mentioned above may be made available immediately for worldwide access unless an embargo applies.

I retain all other ownership rights to the copyright of my work. I also retain the right to use in future works (such as articles or books) all or part of my work. I understand that I am free to register the copyright to my work.

**REVIEW, APPROVAL AND ACCEPTANCE**

The document mentioned above has been reviewed and accepted by the student's advisor, on behalf of the advisory committee, and by the Director of Graduate Studies (DGS), on behalf of the program; we verify that this is the final, approved version of the student's thesis including all changes required by the advisory committee. The undersigned agree to abide by the statements above.

Robert B. McCray, Student

Dr. Braden T. Lusk, Major Professor

Dr. Zach Agioutantis, Director of Graduate Studies

---

UTILIZATION OF A SMALL UNMANNED AIRCRAFT SYSTEM FOR  
DIRECT SAMPLING OF NITROGEN OXIDES PRODUCED BY  
FULL-SCALE SURFACE MINE BLASTING

---

THESIS

---

A thesis submitted in partial fulfillment of the requirements for the  
degree of Master of Science in Mining Engineering in the College  
of Engineering at the University of Kentucky

By

Robert Brendan McCray

Lexington, Kentucky

Director: Dr. Braden T. Lusk, Professor of Mining Engineering

Lexington, Kentucky

2016

Copyright © Robert Brendan McCray 2016

## ABSTRACT OF THESIS

### UTILIZATION OF A SMALL UNMANNED AIRCRAFT SYSTEM FOR DIRECT SAMPLING OF NITROGEN OXIDES PRODUCED BY FULL-SCALE SURFACE MINE BLASTING

Emerging health concern for gaseous nitrogen oxides ( $\text{NO}_x$ ) emitted during surface mine blasting has prompted mining authorities in the United States to pursue new regulations.  $\text{NO}_x$  is comprised of various binary compounds of nitrogen and oxygen. Nitric oxide (NO) and nitrogen dioxide ( $\text{NO}_2$ ) are the most prominent. Modern explosive formulations are not designed to produce  $\text{NO}_x$  during properly-sustained detonations, and researchers have identified several causes through laboratory experiments; however, direct sampling of  $\text{NO}_x$  following full-scale surface mine blasting has not been accomplished.

The purpose of this thesis was to demonstrate a safe, innovative method of directly quantifying  $\text{NO}_x$  concentrations in a full-scale surface mining environment. A small unmanned aircraft system was used with a continuous gas monitor to sample concentrated fumes. Three flights were completed – two in the Powder River Basin. Results from a moderate  $\text{NO}_x$  emission showed peak NO and  $\text{NO}_2$  concentrations of 257 ppm and 67.2 ppm, respectively. The estimated  $\text{NO}_2$  presence following a severe  $\text{NO}_x$  emission was 137.3 ppm. Dispersion of the gases occurred over short distances, and novel geometric models were developed to describe emission characteristics. Overall, the direct sampling method was successful, and the data collected are new to the body of scientific knowledge.

**KEYWORDS:** Nitrogen Oxides, Explosive Gases, Surface Mine Blasting, Small Unmanned Aircraft System, Gas Monitoring

Robert Brendan McCray

---

07/30/2016

---

UTILIZATION OF A SMALL UNMANNED AIRCRAFT SYSTEM FOR  
DIRECT SAMPLING OF NITROGEN OXIDES PRODUCED BY  
FULL-SCALE SURFACE MINE BLASTING

By

Robert Brendan McCray

Dr. Braden T. Lusk

---

Director of Thesis

Dr. Zach Agioutantis

---

Director of Graduate Studies

07/30/2016

---

## DEDICATION

I dedicate this thesis to the cause of human health and safety. It is my hope that the information presented in this document will be used constructively and responsibly for the advancement of public welfare.

## ACKNOWLEDGEMENTS

I want to express my sincere thanks to my wife, Jacquelyn, for her love and support during my time in graduate school. Thanks also to my parents, Robert and Brenda, who encouraged me to pursue an advanced degree.

I am exceptionally grateful for the leadership and guidance of my advisor, Dr. Braden Lusk, who has continuously supported and encouraged me since we met several years ago. In addition, I want to recognize Dr. Josh Calnan, who provided timely assistance with this project. Thanks also to both Dr. Kyle Perry and Dr. Jhon Silva, who challenged me academically and provided excellent suggestions as committee members.

I am very appreciative of Nelson Brothers, LLC and Arch Coal Company, which agreed to contribute time and space for research in pursuit of knowledge and the cause of health and safety. Thanks to Mike Curtis and Dugan Nelson of Nelson Brothers, and also Tim Zeli of Arch Coal, for committing their own individual time toward the completion of this project.

## TABLE OF CONTENTS

ACKNOWLEDGEMENTS .....	iii
LIST OF TABLES .....	vi
LIST OF FIGURES .....	vii
Chapter One: Introduction .....	1
Chapter Two: Review of Literature .....	3
2.1 Assessment of Blast-generated NO <sub>x</sub> .....	3
2.2 Sources of NO <sub>x</sub> .....	6
2.3 Evaluating Cloud Dispersion .....	11
2.4 Relevant Occupational Health Standards and Epidemiology of NO <sub>2</sub> .....	14
2.5 Relevant Air Quality Standards .....	17
2.6 History of Casualties Caused by Blast-generated Gases .....	18
Chapter Three: Summary of Proposed Concept .....	21
Chapter Four: Powder River Basin Sampling.....	23
4.1 Overview.....	23
4.2 Instrumentation .....	24
4.3 Methodology, Flight A.....	32
4.4 Methodology, Flight B.....	35
4.5 Sampling Results, Flight B .....	44
Chapter Five: Additional Sampling .....	47
5.1 Overview.....	47
5.2 Methodology, Flight C.....	47
5.3 Sampling Results, Flight C .....	50
Chapter Six: Blast-generated Cloud Dispersion .....	52
6.1 Overview.....	52
6.2 Cloud Dispersion Results, Flight B .....	52
6.3 Cloud Dispersion Results, Flight C .....	59
Chapter Seven: Health Implications .....	63
7.1 Overview.....	63
7.2 Mine Employee Health .....	64
7.3 Public Health.....	68
Chapter Eight: Challenges of Utilizing an sUAS for NO <sub>x</sub> Sampling .....	70

8.1 Complicated FAA Restrictions .....	70
8.2 Weather Limitations.....	71
8.3 Seasonal Impact on Gas Monitor Usage.....	71
8.4 Gas Monitor Calibration and Upkeep.....	72
8.5 Drone Reliability/Maintenance.....	73
8.6 Distraction for Mine Employees.....	73
8.7 Encouragement of Poor Decision-making.....	73
Chapter Nine: Proposed Alterations to Methodology.....	75
9.1 Overcoming Depth Perception Issues.....	75
9.2 Improving Sampling.....	76
Chapter Ten: Conclusion .....	78
Appendix.....	81
References.....	83
Vita.....	87

## LIST OF TABLES

Table 2.1: Laboratory Testing, Volume of NO <sub>x</sub> per Kilogram of Blasting Agent .....	9
Table 2.2: Guide for Human Exclusion Distance from Blasting (QG, 2011).....	12
Table 2.3: Toxicity Measures of NO <sub>2</sub> , NO, and CO.....	14
Table 2.4: Air Quality Index for Atmospheric NO <sub>2</sub> (EPA, 2006 and EPA, 2011).....	17
Table 4.1: Sensors Installed During Sampling .....	28

## LIST OF FIGURES

Figure 2.1: Sample Standardized Color Chart (AEISG, 2011).....	4
Figure 2.2: Sample Fume Reference (AEISG, 2011) .....	5
Figure 2.3: Effect of ANFO Fuel Oil % on NO <sub>x</sub> (Rowland and Mainiero, 2000).....	7
Figure 2.4: Relevant Estimates of Blast-generated NO <sub>x</sub> .....	10
Figure 4.1: S1000+ (1) Collapsed and (2) Ready for Operation (DJI Innovations) .....	24
Figure 4.2: DJI S1000+ Equipped with Flight Electronics.....	25
Figure 4.3: Battery Tray With Gimbal Attachment Below.....	26
Figure 4.4: Futaba 14SGA, 2.4 GHz Radio Controller and Video Monitor Attachment .	26
Figure 4.5: iBrid MX6 Gas Monitor, Aspirator Model (Industrial Scientific) .....	28
Figure 4.6: Fully Equipped S1000+ (Front View).....	31
Figure 4.7: Flight A Blast-generated Cloud.....	32
Figure 4.8: Flight A Schematic .....	33
Figure 4.9: Full Throttle Acceleration of S1000+ .....	35
Figure 4.10: Flight B Blast-generated Cloud, 30 Seconds Post-blast.....	36
Figure 4.11: Flight B Bench Face Emissions.....	37
Figure 4.12: Flight B Launch Point .....	38
Figure 4.13: Flight B Gas Monitor Activation.....	39
Figure 4.14: S1000+ Hovering with Suspended Tubing .....	40
Figure 4.15: Flight B Blast Sequence .....	41
Figure 4.16: Flight B Schematic .....	41
Figure 4.17: Course Lock Flight Behavior (DJI Wiki, Intelligent Orientation Control)..	42
Figure 4.18: Course Lock Flight Behavior (DJI Wiki, Intelligent Orientation Control)..	42
Figure 4.19: Flight B Landing .....	44
Figure 4.20: Immediate NO <sub>x</sub> and CO Concentrations .....	45
Figure 4.21: GoPro Video Frame Sequence .....	45
Figure 5.1: Flight C Blast-generated Cloud.....	47
Figure 5.2: Flight C Schematic .....	48
Figure 5.3: Flight C Blast-generated Cloud Overhead .....	49
Figure 5.4: NO <sub>2</sub> Measurements 15,000 Feet Downwind.....	50
Figure 6.1: Sampling Near Cloud Periphery in Downwind Direction.....	53

Figure 6.2: Flight B Dispersion Image Sequence .....	54
Figure 6.3: Flight B Geometric Dispersion Model .....	55
Figure 6.4: Flight B Geometric Dispersion of NO <sub>x</sub> .....	57
Figure 6.5: Relevant Estimates of Blast-generated NO <sub>x</sub> Updated .....	58
Figure 6.6: Flight C Geometric Dispersion Model .....	60
Figure 6.7: Flight C Geometric Dispersion of NO <sub>x</sub> .....	61

## Chapter One: Introduction

In February of 2015, the Office of Surface Mining Reclamation and Enforcement (OSM) announced its intention to develop regulations limiting certain toxic gases produced during surface mine blasting. The decision was stimulated by a petition filed in April of 2014 by the environmental group, WildEarth Guardians (WEG). In its appeal, WEG called on OSM to promulgate legislation prohibiting visible emissions of nitrogen oxides (NO<sub>x</sub>), arguing that such emissions pose an immediate risk to human health and safety and universally exceed the Environmental Protection Agency's national ambient air quality standards – causes relevant to the protection granted by the Surface Mining Control and Reclamation Act of 1977 (SMCRA)<sup>1,2</sup>. WEG identified the current lack of NO<sub>x</sub> legislation as a “regulatory gap” and petitioned for “enforceable standards” (WEG, 2014a).

Blasting is an integral part of the surface mining process. Explosive products fracture rock with rapidly-expanding gases. The volume of gas produced during a blast is typically 1,000 times that of the original explosives product (QG, 2011). Various non-ideal circumstances can degrade an explosive reaction and form unintended, toxic byproducts. Nitrogen-based explosives (particularly ANFO) have the potential to generate NO<sub>x</sub> when an imperfect explosive reaction occurs. Of the various nitrogen oxides, nitric oxide (NO) and nitrogen dioxide (NO<sub>2</sub>) are the most prevalent and hazardous in the blasting context. NO<sub>2</sub> is of greater toxicity than NO and is a skin, eye, and lung irritant. Concentrated doses can lead to illness or death, though the relevant histories of such events in the mining and

---

<sup>1</sup> Section 102(a) describes one of SMCRA's goals as “protecting society and the environment from the adverse effects of surface coal mining operations” (95<sup>th</sup> Congress, 1977).

<sup>2</sup> Section 515(b)(15)(C)(i)-(ii) states that blasting activities should be limited in order to “prevent injury to persons [and] damage to public and private property outside the permit area” (95<sup>th</sup> Congress, 1977).

commercial explosives industries are small. Most accidents resulting from blasting emissions have been caused by carbon monoxide (CO), which can become a health issue following confined blasting – if the gas migrates through strata to nearby surface structures.

Gases produced during surface blasting are typically concentrated in a “cloud” or “fume.” Dispersion of a cloud usually occurs within a short time, as the prevailing wind transports it from the blast site; however, it is possible for clouds to be (1) contained within the blast site if the explosives are detonated in a confined area (such as a pit) or (2) carried across the permit boundary if the blast occurs near the boundary or is of considerable scale.

Currently, the NO<sub>x</sub> concentration present in blast-generated clouds is understood qualitatively by cloud coloration – yellow, orange, red, and brown. There have been few attempts to acquire direct, physical measurements from blast-generated clouds to represent the various observed colors. Risk of exposure to concentrated, harmful gases (such as NO<sub>x</sub>), heavy dust, and distance to the shot (typically >1,000 feet for safety from fly material) limit effective gas sampling options.

The purpose of this project is to demonstrate a safe, innovative method of directly quantifying NO<sub>x</sub> concentrations generated by full-scale surface mine blasting. A small unmanned aircraft system (sUAS) and continuous gas monitor are used to collect measurements. Experimental results contribute to the body of knowledge regarding blast-generated NO<sub>x</sub>, advance the scientific understanding of blasting’s immediate impact on the local atmosphere, and offer objective insight into the extent of human health risk.

## **Chapter Two: Review of Literature**

### **2.1 Assessment of Blast-generated NO<sub>x</sub>**

Previous studies evaluating explosive-generated NO<sub>x</sub> have primarily been conducted in isolated blasting chambers or controlled-volume facilities. Experiments by Chaiken et al. (1974), Mainiero (1997), Rowland and Mainiero (2000), Rowland et al. (2001), and Sapko et al. (2002) measured the small-scale NO<sub>x</sub> output of the most widely-used explosives products, including ANFO, emulsion, and ANFO/emulsion blends. These same experiments evaluated some of the potential sources of NO<sub>x</sub>, discussed in Section 2.2.

Few studies have attempted to measure NO<sub>x</sub> following full-scale surface mine blasting, primarily due to practical difficulties involved with prediction of the cloud path and retrieval of representative samples. Attalla et al. (2008) published a paper describing an indirect method quantifying NO<sub>x</sub> inside of blast-generated clouds using ultraviolet spectrometry. The data were supplemented by ground-level gas monitor readings collected downwind. The evaluation focused on NO<sub>2</sub> and concluded that the gas was present in observed clouds between 0 and 7 ppm, with a maximum recorded value of 17 ppm.

At this time, there are no physical data available that can adequately quantify the instantaneous peak NO<sub>x</sub> concentrations within blast-generated clouds. For this reason, NO<sub>x</sub> presence is visually classified in a qualitative manner. It is generally accepted that low NO<sub>x</sub> concentrations are associated with pale yellow, high with dark red or purple, and intermediate with various intensities of orange (WEG, 2014a; QG, 2011; and AEISG, 2011). The color of the cloud is the result of NO<sub>2</sub> alone. According to the Queensland State Government, 2.5 ppm NO<sub>2</sub> is the minimum visible concentration (WEG, 2014b). The

Australian Explosives Industry and Safety Group Inc. (AEISG) has developed a standardized, qualitative color chart for describing blast-generated NO<sub>x</sub> (Figure 2.1). The chart is one of few published NO<sub>x</sub> management techniques in the mining and commercial explosives industries.

<b>Fume Level</b>	<b>Color</b>	<b>Pantone Number</b>
Level 0 No NO <sub>x</sub> gas		Warm Grey 1C (RGB 244, 222, 217)
Level 1 Slight NO <sub>x</sub> gas		Pantone 155C (RGB 244, 219, 170)
Level 2 Minor yellow/orange gas		Pantone 157C (RGB 237, 160, 79)
Level 3 Orange gas		Pantone 158C (RGB 232, 117, 17)
Level 4 Orange/red gas		Pantone 1525C (RGB 181, 84, 0)
Level 5 Red/purple gases		Pantone 161C (RGB 99, 58, 17)

Figure 2.1: Sample Standardized Color Chart (AEISG, 2011)

Figure 2.2 provides a visual reference to levels one through five of the AEISG color chart. The letter code assigned to a particular fume level in Figure 2.2 refers to the extent of NO<sub>x</sub> produced across the blasting pattern. Localized refers to only a few blast holes, Medium refers to 50% of the holes, and extensive indicates that all blast holes are responsible for the emission (AEISG, 2011).

Level	Typical Appearance
<b>Level 0</b> No NOx gas	
<b>Level 1</b> Slight NOx gas	
1A Localised	
1B Medium	
1C Extensive	
<b>Level 2</b> Minor yellow/orange gas	
2A Localised	
2B Medium	
2C Extensive	
<b>Level 3</b> Orange gas	
3A Localised	
3B Medium	
3C Extensive	
<b>Level 4</b> Orange/red gas	
4A Localised	
4B Medium	
4C Extensive	
<b>Level 5</b> Red/purple gas	
5A Localised	
5B Medium	
5C Extensive	

Figure 2.2: Sample Fume Reference (AEISG, 2011)

## 2.2 Sources of NO<sub>x</sub>

Potential sources of NO<sub>x</sub> have been identified through laboratory studies. The following list represents a thorough (but not necessarily comprehensive) collection of factors that affect an explosive's performance (QG, 2011):

- 1) Manufacture and specification of explosive ingredients
- 2) Explosive mixture (e.g. under-fueled ANFO)
- 3) Density of loaded explosives
- 4) Degree of confinement
- 5) Water damage
- 6) Ground conditions (cracks, voids, etc.) that affect planned loading practices
- 7) Borehole loading practices

ANFO is most commonly associated with NO<sub>x</sub> production, though past experiments have explored the relationships between ANFO, emulsion, and various blends of the two agents.

Early work by Chaiken et al. (1974) tested ANFO mixtures within the Bureau of Mines closed gallery facility. Findings showed that under-fueled ANFO produced increased volumes of NO<sub>x</sub>. Later work by Mainiero (1997) and Rowland and Maniero (2000) monitored the detonation of various mixtures of ANFO in the National Institute for Occupational Safety and Health's Pittsburgh Research Laboratory. Results indicated that a mixture of 94% ammonium nitrate and 6% fuel oil was close to optimum for minimizing the volume of NO<sub>x</sub> generated. Figure 2.3 displays relevant data collected by Rowland and Mainiero (2000) and demonstrates the trend in NO<sub>x</sub> and NO<sub>2</sub> by fuel oil content.

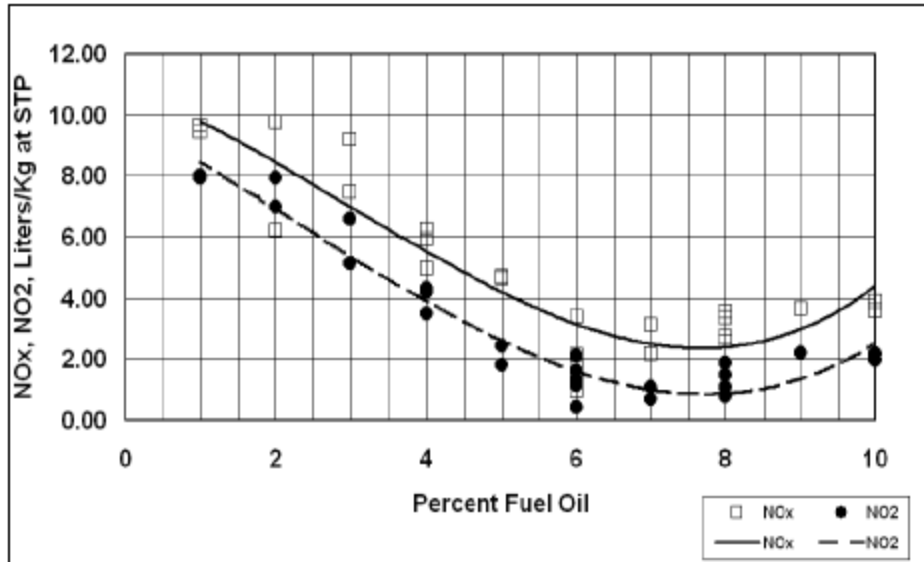


Figure 2.3: Effect of ANFO Fuel Oil % on NO<sub>x</sub> (Rowland and Mainiero, 2000)

Rowland and Mainiero (2000) also evaluated the effect of water content (i.e. water damage) on NO<sub>x</sub> generation. Figure 2.4 identifies a generally-increasing trend in NO<sub>x</sub> production as ANFO (6% fuel oil) is exposed to larger concentrations of water.

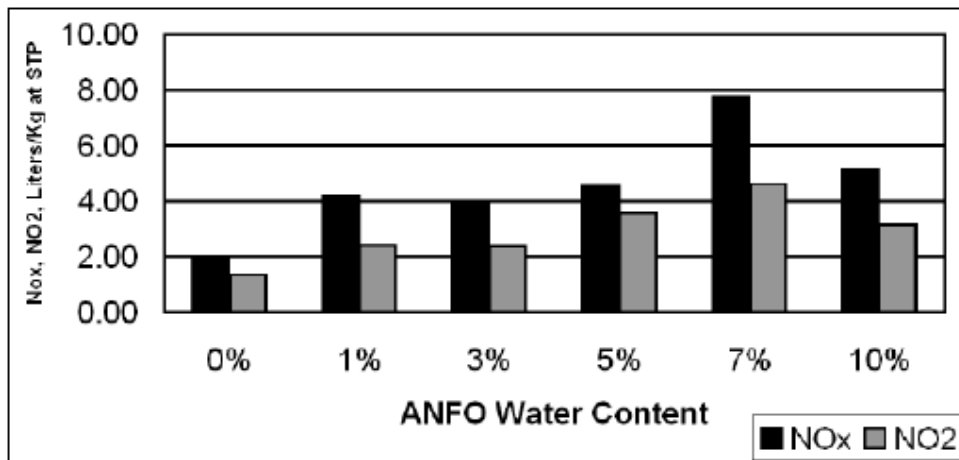


Figure 2.4: Effect of ANFO Water Content on NO<sub>x</sub> (Rowland and Mainiero, 2000)

Other notable findings by Rowland and Mainiero (2000) included testing of aluminum and rock dust additives in 6% fuel oil ANFO mixtures. The presence of aluminum did not increase NO<sub>x</sub> emissions; however, rock dust did. The results indicated that that drill cutting contamination in explosives (i.e. rock dust) influenced the quality of detonation.

Rowland et al. (2001) assessed the NO<sub>x</sub> production of emulsion and ANFO/emulsion blends at the Pittsburgh Research Laboratory. The authors specifically examined the effect of relative confinement, using schedule 80 steel pipe and galvanized sheet metal pipe. In addition, samples were exposed to various intervals of water exposure to explore degradation of explosive mixtures over time. The water component of the experiment was tuned to address conclusions presented by Schettler and Brasher (1996), which stated that an ANFO/emulsion blend was only water-resistant with 40% or greater emulsion content and water-proof with at least 50% emulsion. Results presented by Rowland et al. (2001) agreed with the previous evidence, showing that water introduced to a 70/30 ANFO/emulsion blend for one day prevented detonation and any water exposure of the blend within the galvanized sheet metal pipe completely inhibited detonation. Furthermore, the 50/50 blends were water resistant for short-term exposures up to one week. Pure emulsion detonated even after two months. It was noted that, while there was no substantial deviance in detonation velocity, and the physical appearance of the agent appeared normal after two months, NO<sub>x</sub> production was higher than anticipated.

Sapko et al. (2002) conducted a series of controlled tests designed to evaluate ANFO particle size, inexpensive additives, relative confinement, critical diameter, water stemming, oil wicking, and detonation within an air-displaced atmosphere. The authors compared NO<sub>x</sub> volumes generated by ANFO, emulsion, and a 50/50 blend in the Pittsburgh

Research Laboratory. Findings showed that lower relative confinement, fuel oil wicking by dry/soft/porous soil during extended sleep times (especially in small boreholes), ANFO water damage, and drill cutting contamination in emulsion increased NO<sub>x</sub>. In addition, the various additives (urea, coal dust, aluminum powder, excess fuel oil) reduced NO<sub>x</sub>.

The laboratory testing previously described is organized by author in Table 2.1. It lists the lowest and highest volumes generated per kilogram of blasting agent. If no range was provided by a particular author, point estimates are listed (Chaiken et al., 1974 and EPA, 1980). The concept for this tabular organization was derived from a report published by Lashgari et al. (2013), which evaluated mine-wide environmental NO<sub>x</sub> emissions from equipment and blasting.

Table 2.1: Laboratory Testing, Volume of NO<sub>x</sub> per Kilogram of Blasting Agent

<b>AUTHOR</b>	<b>AGENT</b>	<b>CONDITION</b>	<b>NO<sub>x</sub> (L/kg)</b>
Chaiken et al. (1974)	ANFO	Under fueled	7.0
Environmental Protection Agency	ANFO	1980 Published Estimate	5.8
Mainiero (1997)	ANFO	Low, 94/6 product	2.5
		High, under fueled	4.8
Rowland and Mainiero (2000)	ANFO	Low, 0% Water, 94/6	2.0
		High, under fueled, 99/1	9.9
Rowland et al. (2001)	Emulsion	Low, no water	2.7
		High, one week water	6.5
	50/50	Low, steel pipe, one week water	5.0
		High, steel pipe, one month water	11.8
Sapko et al. (2002)	ANFO	Low, steel pipe confinement	11.0
		High, galv. steel pipe confinement	36.5
	Emulsion	Low, steel pipe confinement	4.2
		High, drill cuttings contamination	6.2
	50/50	Low, steel pipe confinement	19.6
		High, galv. steel pipe confinement	31.0

Figure 2.4 provides an improved graphical representation of the various ranges and point estimates presented in Table 2.1.

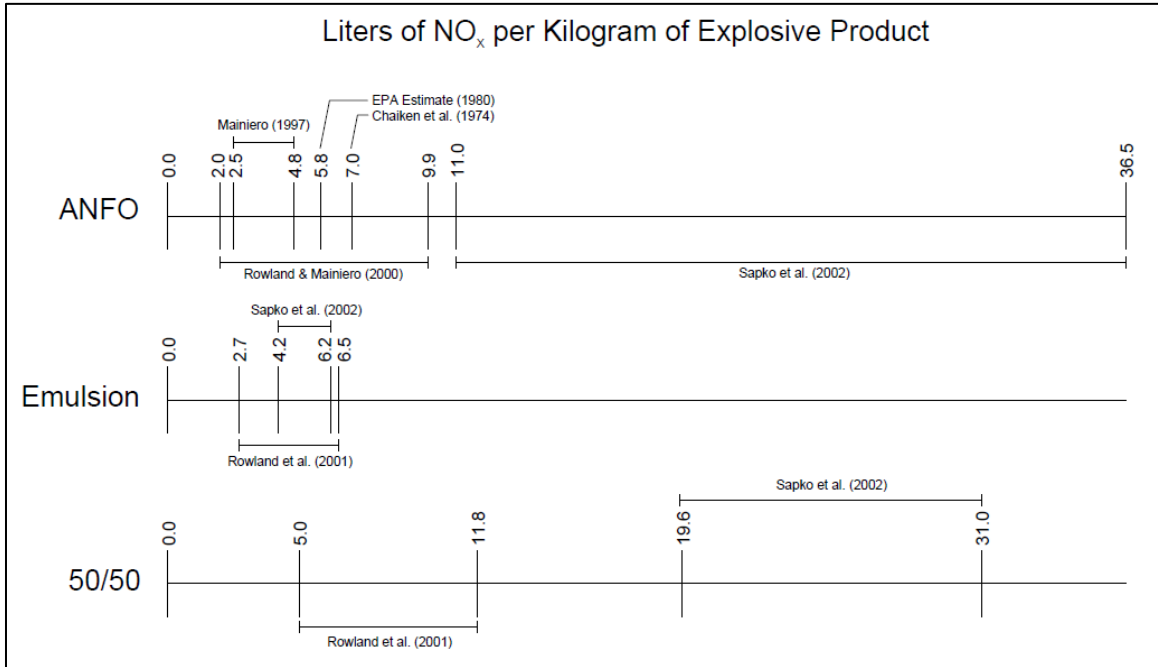


Figure 2.4: Relevant Estimates of Blast-generated NO<sub>x</sub>

Based on existing research, it is clear from Figure 2.4 that ANFO and 50/50 ANFO/emulsion blends are expected to generate elevated volumes of NO<sub>x</sub> compared to pure emulsion. Emulsion naturally has water resistance by its composition, providing some explanation for the narrow range of NO<sub>x</sub> generated per kilogram of the explosive. In addition, Sapko et al. (2002) suggested that another specification of emulsion is also influential. Specifically, the difference in grain size between ANFO and emulsion. According to the authors, Ammonium nitrate prills in ANFO are relatively large. Alternatively, the nitrate component of emulsion is in solution, allowing for enhanced contact with the emulsified fuel. The detonation of emulsion therefore facilitates immediate reactions of NO<sub>x</sub> with hydrocarbons, generating more nitrogen and water instead of NO.

### 2.3 Evaluating Cloud Dispersion

*Cloud Dispersion* is the natural dilution of toxic gaseous components to safe or ambient atmospheric concentrations.  $\text{NO}_x$  generated by surface blasting typically disperses in seconds to minutes, depending on the scale of emissions, local atmospheric conditions, and initial toxicity of the cloud (Sapko et al, 2002; AEISG, 2011; and QG, 2011). The cloud dispersion rate directly affects human health and safety, since concentrations of NO and/or  $\text{NO}_2$  may remain sufficiently high for a short period after a blast to harm individuals in the cloud path (AEISG, 2011). There are few examples of formal cloud dispersion analyses, but those available have applied computer-based dispersion modeling techniques.

Attalla et al. (2008) utilized AFTOX to evaluate whether concentrations of  $\text{NO}_2$  from observed blasting emissions were unhealthy at five kilometers downwind. The findings suggested that  $\text{NO}_2$  levels at this distance and beyond “may be indistinguishable from background levels; typically of the order of several parts per billion, in most cases” (Attalla et al., 2008). AFTOX is a toxic chemical dispersion model developed by the United States Air Force. It is a Gaussian dispersion model designed for continuous or instantaneous emissions of liquids or gas from a single location (plume emissions). AFTOX can be used to calculate a toxic corridor (hazardous concentration by distance from the source), the concentration at a specific location, or the maximum concentration and its associated location (Kunkel, 1991 and Dungey, 1993).

The Queensland Government in Australia (QG, 2011) developed a human exclusion zone as a guide to protect individuals from  $\text{NO}_2$  concentrations above 5.0 ppm. The exclusion zone was defined using SLAB modelling software. SLAB is an atmospheric dispersion

model for denser-than-air plume releases, such as blast-generated NO<sub>2</sub>. It calculates dispersion by solving for conservation of mass, momentum, energy, and species. The model was developed at the Lawrence Livermore National Laboratory (Ermak, 1990). Table 2.2 is a reconstruction of the human exclusion table produced by QG (2011). Exclusion distances downwind and crosswind from blasting are derived from the fume level (i.e. a specific initial NO<sub>2</sub> concentration) and local atmospheric wind conditions.

Table 2.2: Guide for Human Exclusion Distance from Blasting (QG, 2011)

Fume Category (subjective ranking)	Initial NO <sub>2</sub> (ppm)	Downwind Exclusion Distance (m) Required to Maintain NO <sub>2</sub> Below 5.0 ppm				Potential Extent of 0.12 ppm (m) (odor threshold)	Crosswind Exclusion Distance (m) (from blast cloud center line)
		Stability Class and Wind Speed					
		A (very unstable) High Temp, Windy	B (unstable)	C (slightly unstable)	D (neutral)		
		Wind Speed 6.8 - 12.6 kmph (4.2 - 7.8 mph)	Wind Speed 2.9 - 10 kmph (1.8 - 6.2 mph)	Wind Speed 1.4 - 4.32 kmph (0.9 - 2.7 mph)	Wind Speed 1.4 - 2.2 kmph (0.9 - 1.4 mph)		
0	2	100	100	100	100	1,200	100
1	4	130	140	150	150	3,000	150
2	7	400	500	500	500	4,000	500
3	17	600	1,000	1,200	1,200	8,000	1,000
4	70	900	1,600	3,000	3,000	13,000	1,500
5	500	1,600	3,000	5,000	5,000	20,000	2,000

Table 2.2 is one of few published dispersion tools and is burdened by limited data and a number of critical assumptions, including the following (QG, 2011):

1. Initial clouds are universally 100 meters by 100 meters in size and extend from the ground vertically to 150 meters.
2. The surface roughness applied in the model is 0.05 meters, representative of a grassland landscape
3. Up to five times NO<sub>2</sub> may appear through oxidation of NO to NO<sub>2</sub> during dispersion.

Assumption three is a major uncertainty. Oxidation of NO to NO<sub>2</sub> occurs naturally in air, since NO is unstable in the presence of oxygen and moisture (Wieland 1998 and Onederra 2012). Oxidation occurs through the following chemical reaction:



The rate of oxidation depends on the initial NO concentration and time (Sapko et al., 2002). Mainiero et al. (2006) examined the kinetics of oxidation for NO as a gaseous detonation product, finding a consistent rate constant for concentrations of NO up to 100 ppm (Mainiero et al., 2006). As a result of oxidation, the immediate, post-blast NO<sub>2</sub> concentration may be the largest measurable, but more of the gas will form as the cloud is in transit and dispersing.

In addition to Attalla et al. (2008) and QG (2011), The United States Bureau of Land Management (BLM, 2010) referenced an unspecified NO<sub>x</sub> modelling method in its comprehensive environmental impact statement for the Wright, Wyoming area coal lease applications. According to the publication, air quality permit applications submitted by the Black Thunder, Jacobs Ranch, and North Antelope Rochelle mines were evaluated, in order to assess the worst-case annual NO<sub>x</sub> emissions (blasting and other sources). The indirect modelling analysis by the BLM found that “impacts from the worst case years fall well below the annual NO<sub>2</sub> NAAQS of 100 µg/m<sup>3</sup>” (BLM, 2010). NAAQS refers to the National Ambient Air Quality Standards, set forth by the Environmental Protection Agency (EPA, 2011). The secondary standard requires an average atmospheric NO<sub>2</sub> concentration of at most 53 ppb over one year, as codified in 40 CFR 50.11 (see Section 2.5 for further information).

## 2.4 Relevant Occupational Health Standards and Epidemiology of NO<sub>2</sub>

The Occupational Safety and Health Administration (OSHA), American Conference of Governmental Industrial Hygienists (ACGIH), and National Institute for Occupational Safety and Health (NIOSH) have published standards regarding human exposure to NO and NO<sub>2</sub>. Table 2.3 displays the current OSHA regulatory exposure limits, in addition to those suggested by ACGIH and NIOSH (OSHA, n.d.; ACGIH, 2012; NIOSH, 1995).

Table 2.3: Toxicity Measures of NO<sub>2</sub>, NO, and CO

SUBSTANCE	OSHA REGULATORY PEL <sup>(A)</sup>	ACGIH TLV <sup>(B)</sup>	NIOSH REL <sup>(C)</sup>	NIOSH IDLH <sup>(D)</sup>
Nitrogen Dioxide	5 ppm Ceiling	0.2 ppm TWA	1 ppm STEL	20 ppm
Nitric Oxide	25 ppm TWA	25 ppm TWA	25 ppm TWA	100 ppm
Carbon Monoxide	50 ppm TWA	25 ppm TWA	35 ppm TWA; 200 ppm Ceiling	1,200 ppm

<sup>(A)</sup> PEL: Permissible exposure limit – defined as either (1) an 8-hour time-weighted average, (2) a 15 minute short term exposure limit, or (3) a ceiling exposure concentration

<sup>(B)</sup> TLV: Threshold limit value – see PEL

<sup>(C)</sup> REL: Recommended exposure limit – see PEL

<sup>(D)</sup> IDLH: Immediately dangerous to life or health concentration

NO<sub>2</sub> is a more prominent health concern than NO, as demonstrated by Table 2.3. NO<sub>2</sub> is a corrosive, reactive gas that has a strong odor. According to NIOSH (1979), symptoms of acute exposure vary, based on the duration and concentration. Minor exposures can result in irritation of the skin, eyes, and nose, in addition to coughing, shortness of breath, and headaches. Exposure for extended time periods or to elevated concentrations can cause *pulmonary edema*, a severe and often fatal outcome that congests the lungs with fluid. The exact duration and/or concentration of NO<sub>2</sub> that produce pulmonary edema are not defined, but it is known that a latency period of 3 to 30 hours exists between initial exposure and onset of symptoms.

OSHA derived its regulatory ceiling limit of 5 ppm from the findings of several epidemiologic studies that assessed human exposure to NO<sub>2</sub>. Douglas et al. (1989) examined the medical outcomes of 17 patients exposed to silo gas (NO<sub>2</sub> generated during natural fermentation of chopped forages) between 1955 and 1987. Of the study group, 11 suffered from acute lung injury, one of whom perished from pulmonary edema. Helleday et al. (1995) assessed the mucociliary activity of 24 healthy individuals in vivo. The subjects were divided into three groups and exposed to either 1.5 ppm NO<sub>2</sub> for 20 minutes, 3.5 ppm NO<sub>2</sub> for 20 minutes, or 3.5 ppm NO<sub>2</sub> for four hours. The authors concluded that “short-term exposure to NO<sub>2</sub> in man produces a significant reduction in the mucociliary activity 45 [minutes] after exposure,” ceasing within 24 hours. Linaker et al. (2000) evaluated the relationship between NO<sub>2</sub> exposure in asthmatic children and post-respiratory-infection airway constriction. Results demonstrated that relatively low concentrations of NO<sub>2</sub> increased the risk of asthmatic exacerbation after respiratory infection. Frampton et al. (2002) studied the cause-effect relationship between exposure to NO<sub>2</sub> and respiratory health. A total of 21 healthy patients were subjected to a range of 0.6 to 1.5 ppm NO<sub>2</sub> for three hours with some exercise. In vitro testing of cells collected via phlebotomy and bronchoscopy revealed a weakened immunity of epithelial cells to respiratory viruses.

NIOSH developed its recommended exposure limit for NO<sub>2</sub> based on an extensive case history of environmental data and epidemiological analyses. Smith (1976) described the criteria relative to the development of the NIOSH standard, which was designed for a 10-hour workday, a 40-hour workweek, and the lifetime of an employee. The report included relevant examples of occupational exposure, animal experimentation, and a small number

human studies that evaluated only low concentrations of NO<sub>2</sub>. It also addressed acute and chronic exposure to NO<sub>2</sub> and provided some discussion of continuous versus intermittent exposure. The findings correlating exposure and effect stated that “the acute and usually delayed effects of higher concentrations of nitrogen dioxide on man are well established.” Eight human case histories demonstrated evidence of delayed onset of pulmonary edema. Several of the afflicted individuals also experienced relapse after recovering from the initial pulmonary edema. Relapse was attributed to *bronchiolitis fibrosa obliterans*, a pathologic lesion of the lung. Conditions relevant to acute pulmonary edema and bronchiolitis fibrosa obliterans were described in the context of the relative NO<sub>2</sub> concentration at exposure:

*[Pulmonary edema and associated relapse events] have not been reported at relatively steady low levels of exposure associated with those few industrial processes in which oxides of nitrogen are steadily generated and get into the workplace atmosphere. All reported cases have arisen as a result of sudden or intermittent emission of oxides of nitrogen from an accidental event such as an explosion or combustion of nitroexplosives, the accidental escape or spilling of concentrated nitric acid, the intermittent process of arc or gas welding, especially in a confined space, or the imprudent entry into an agricultural silo which was not ventilated. (Smith, 1976)*

It was observed by NIOSH that the “characteristic delay” between initial exposure and onset of pulmonary edema was 12 hours (Smith, 1976).

Though not referenced by OSHA or NIOSH, a more recent study published by Hesterberg et al. (2009) examined fifty experimental studies of short-term human inhalation of NO<sub>2</sub>. The authors did not determine a consistent trend in changing lung function or bronchial sensitivity with increasing NO<sub>2</sub> concentrations. It was concluded that “a health-protective, short-term NO<sub>2</sub> guideline level for susceptible (and healthy) populations would reflect a policy choice between 0.2 and 0.6 ppm” (Hesterberg et al., 2009).

## 2.5 Relevant Air Quality Standards

The Environmental Protection Agency (EPA) regulates atmospheric NO<sub>2</sub> under the Clean Air Act, along with four other air pollutants: ground-level ozone, particulate matter, carbon monoxide, and sulfur dioxide (40 CFR § 50-97, 2010). The annual arithmetic average concentration of NO<sub>2</sub> must not exceed 53 ppb. A revision in 2010 included a 1-hour short-term arithmetic average restriction of 100 ppb NO<sub>2</sub> (40 CFR § 50.11, 2010). These limits are referred to as national ambient air quality standards (NAAQS). NAAQS values are designed to combat adverse human health effects of the specified pollutants (EPA, 2011).

The EPA has developed an air quality index (AQI) as a standardized method of reporting polluted atmospheres and identifying sensitive groups. Larger index values indicate a greater health concern. AQI values of 100 are intended to match the NAAQS. Table 2.4 shows the NO<sub>2</sub> AQI, including cautionary statements (EPA 2006 and EPA 2011).

Table 2.4: Air Quality Index for Atmospheric NO<sub>2</sub> (EPA, 2006 and EPA, 2011)

AQI Range	1-Hour NO <sub>2</sub> Average (ppb)	AIR QUALITY	CAUTIONARY STATEMENT
0 - 50	0 - 53	<b>Good</b>	None
51 - 100	54 - 100	<b>Moderate</b>	Unusually sensitive people should consider reducing prolonged or heavy outdoor exertion.
101 - 150	101 - 360	<b>Unhealthy for Sensitive Groups</b>	Active children, the elderly, and people with lung disease, such as asthma, should reduce prolonged or heavy outdoor exertion.
151 - 200	361 - 649	<b>Unhealthy</b>	Active children, the elderly, and people with lung disease, such as asthma, should avoid prolonged or heavy outdoor exertion; everyone else, especially children, should reduce prolonged or heavy outdoor exertion.
201 - 300	650 - 1,244	<b>Very Unhealthy</b>	Active children, the elderly, and people with lung disease, such as asthma, should avoid all outdoor exertion; everyone else, especially children, should avoid prolonged or heavy outdoor exertion.
> 301	> 1,245	<b>Hazardous</b>	Children, the elderly, and people with lung disease, such as asthma, should remain indoors; everyone else, especially children, should avoid outdoor exertion.

The short-term NAAQS for NO<sub>2</sub> is relevant to surface blasting, since clouds have been observed propagating beyond permit boundaries in some instances (Sapko et al., 2002; BLM, 2010). There are few studies that have directly compared the impact of blast-generated NO<sub>x</sub> with public air quality. A thorough search produced only one example. Battelle (2012) prepared an extensive report for the West Virginia Department of Environmental Protection that demonstrated continuous and passive sampling of air pollutants (including NO<sub>2</sub>) in a community neighboring two active surface coal mines. EPA-accepted sampling techniques were applied, in order to evaluate the impact of mine blasting on local air quality. Analysis of readings collected during a two-week period produced the following conclusion: “The overall finding of this study thus is that the local air quality is well within applicable health-based standards and does not appear to be affected by emissions from nearby blasting events in surface coal mining” (Battelle, 2012).

## **2.6 History of Casualties Caused by Blast-generated Gases**

Carbon monoxide has been proven to be responsible for the overwhelming majority of injuries caused by gases generated during surface blasting. An extensive literature base has been dedicated to the dangers of carbon monoxide in the mine blasting context. Researchers have discovered that confined blasting (esp. trench blasting) can suppress the release of gases into the atmosphere, causing gases to migrate through cracks, joints, and other geologic discontinuities (Eltschlager et al., 2001; Santis, 2001; Santis, 2003; Harris et al., 2004; Harris et al., 2005). Between 1988 and 2005, there were 13 documented cases of carbon monoxide propagation through strata into nearby structures (Harris et al., 2005).

Casualties of blast-generated NO<sub>x</sub> have primarily occurred in underground mining. Wieland (1998) reported anecdotally on the dangerous nature of NO<sub>2</sub>, stating: “typical of circumstances was a workman who inhaled dynamite fumes for some time, felt well during the working day, noticing no ill effects that night, only to die the next day of pulmonary edema.” Kennedy (1972) studied 100 underground coal miners over 10 years, all of whom had exposure to “nitrous fumes” from conventional blasting techniques. The author discovered that low exposures over months to years produced an “emphysema-like” health condition, and short-duration exposures to high concentrations caused an acute chest illness with a generally full recovery. Many of the miners experienced pulmonary edema at some point. Peak NO<sub>2</sub> concentrations were measured at 88 ppm and 167 ppm during regular blasting and misfires, respectively (Kennedy, 1972).

Attention has recently shifted to NO<sub>x</sub> generated during surface blasting, though there are few examples of public or mine personnel requiring medical attention because of contact with the gases. OSM documented instances of public exposure to NO<sub>x</sub> from Arch Coal’s Black Thunder Coal Mine in the Powder River Basin prior to 2001, which resulted in special control measures when large overburden shots are planned (BLM, 2010). Mining authorities in Australia reported in 2011 that a two-week period of blasting in intensely saturated ground resulted in the formation of four major clouds. Two clouds forced a total of twenty four surface miners to report to a hospital for NO<sub>x</sub> exposure (Madden, 2011). A thorough examination of literature revealed only one surface mine blasting fatality to be the direct result of post-blast NO<sub>2</sub> exposure. The event occurred in the Philippines in 2006. According to the Queensland Department of Natural Resources and Mines, a blaster was conducting a post-blast inspection at a quarry and fell into a void eight meters deep.

Hospital staff treated him for minor injuries, but his trouble breathing was not properly addressed. The next day, he succumbed to severe pulmonary edema (Madden, 2011). Beyond these examples, blast-generated NO<sub>x</sub> is an obscure health and safety influence in the surface mining context.

WEG expressed the latest concern for NO<sub>x</sub> generated during surface blasting, in its petition to OSM. The organization's inquiry was primarily directed at cast blasting operations, such as those in the Powder River Basin region of the United States (WEG, 2014a). Cast blasting at surface coal mines in the Powder River Basin sometimes detonates up to two million pounds of blasting agent in a single event (Sapko et al., 2002 and Mainiero et al., 2006). The existing body of knowledge regarding blast-generated NO<sub>x</sub> must be expanded, in order to bridge the current knowledge gap and address unanswered questions regarding the initial toxicity of large NO<sub>x</sub> clouds and the nature of their dispersion.

### **Chapter Three: Summary of Proposed Concept**

Direct sampling during the formation and dispersion of blast-generated NO<sub>x</sub> clouds has historically been considered impractical, due to the inherently violent and hazardous nature of mine blasting. Post-blast conditions at mine sites are unsafe because of gas and dust contaminants in the local atmosphere, elevated bench heights, and disturbed geologic environments. Blasters and observers typically also recognize an observation distance of 1,000 feet, as a rule of thumb to remain safe from fly material. The application of small unmanned aircraft system (sUAS) technology is capable of overcoming perceived safety and accessibility challenges.

The primary value of deploying an sUAS is safety. Most modern radio controllers for sUAS permit flight distances up to one mile. For this reason, operators, assistants, and other observers should face no exposure to potentially-harmful, post-blast conditions, and flights can be conducted from a pre-determined location. Safety risks generated by sUAS operations are limited almost exclusively to personnel injury during landing and takeoff; however, such events are preventable with proper standard operating procedures. The sparse mine setting provides an ideal flight location for remote operated aircraft.

Rotorcraft sUAS are specifically capable of facilitating accessibility to NO<sub>x</sub> clouds during both formation and dispersion. Many rotorcraft can achieve speeds between 20 and 45 miles per hour. As a result, intercepting a cloud is possible within seconds. The machines can be repositioned dynamically and, through GPS guidance, are capable of hovering at a stationary location. Unique flight modes also provide control options that are not available with fixed-wing sUAS. Flight modes are described in Sections 4.2, 4.3, and 5.2.

Overall, remote operation of rotorcraft sUAS offers an efficient method of evaluating (1) the immediate impact of surface mine blasting on the local atmosphere, (2) the dissipation of blast-generated clouds, and (3) oxidation of NO to NO<sub>2</sub> in a full-scale mining environment. The purpose of the following sections is to establish this novel sampling method and demonstrate practical results.

## Chapter Four: Powder River Basin Sampling

### 4.1 Overview

Two flights were completed in the Powder River Basin. These flights are referred to as Flight A and Flight B and are summarized below:

- Flight A occurred at the Black Thunder Coal Mine, operated by Arch Coal. The designated takeoff and landing location was approximately 2,000 feet from the blast. The challenge of depth perception in the large open space, in addition to poor weather conditions (rain with wind gusts exceeding 20 miles per hour), did not allow the S1000+ to come into contact with the blast-generated cloud. It is believed that NO<sub>x</sub> was present in one area of the cloud, but no useful data was collected.
- Flight B occurred at the Coal Creek Mine, operated by Arch Coal. The designated takeoff and landing location was about 1,000 feet from the nearest row of holes. The shot was an overburden blast (not a cast panel), containing approximately 330,432 pounds of explosives. Informative data regarding instantaneous concentrations of NO, NO<sub>2</sub>, and CO was collected successfully.

Section 4.2 describes the instrumentation used to capture gas readings, along with relevant technical specifications. Section 4.3 describes the individual methodologies applied in the field during both Flight A and Flight B, including pre-blast decision-making and in-flight sampling strategy. Section 4.4 illustrates the gas sample collected during Flight B.

The established qualitative color scale interpretation of NO<sub>x</sub> (Figure 2.2) is used to assign fume levels to the observed blast-generated clouds. The fume level classifications are intended to supplement gas monitor readings by addressing the suspected intensity of NO<sub>x</sub> that is assumed from a purely visual observation.

## 4.2 Instrumentation

The sUAS deployed during testing was a DJI S1000+, manufactured by DJI Innovations. The S1000+ is a rotorcraft, with eight motors arranged in a circular pattern. The motors are positioned at the end of foldable arms. The full diameter of the machine is four feet, when the arms are raised and locked into position. Figure 4.1 shows the sUAS carbon fiber frame without any of the flight electronics, battery, or attachments.



Figure 4.1: S1000+ (1) Collapsed and (2) Ready for Operation (DJI Innovations)

The S1000+ was selected because of its flight capabilities and weight capacity. Pre-programmed flight modes permit either rectangular navigation or radial turning about the takeoff location. It is able to cover a large area quickly, achieving a maximum horizontal speed of 45 miles per hour. The flight system can be operated manually via radio controller, or a predetermined flight path can be uploaded and traversed autonomously with precision. In large open spaces, the flight controller self-corrects in response to adverse conditions,

such as variable wind speed and direction (recommended maximum of 20 mph). The S1000+ can function properly with an all-inclusive takeoff weight of 24 pounds.

Figure 4.2 shows the experimental S1000+ and its necessary flight electronics. Rotor blades and the antenna are collapsed in the image.



Figure 4.2: DJI S1000+ Equipped with Flight Electronics

Major components of the S1000+ were assembled by third-party sUAS professionals. Sensitive electronic components were fastened further using adhesive Velcro strips. A Zenmuse H4-3D gimbal with three axes of stabilization was also installed below the battery tray, as displayed in Figure 4.3.



Figure 4.3: Battery Tray With Gimbal Attachment Below

A GoPro Hero4 camera was bound to the gimbal. 4K resolution was used exclusively during experimentation to capture the highest-resolution video possible. The camera was charged during flight by built-in electronics, and a live video feed was provided to a video monitor attached to the radio controller, displayed in Figure 4.4.



Figure 4.4: Futaba 14SGA, 2.4 GHz Radio Controller and Video Monitor Attachment

The selected Futaba controller is rated for flight operations up to one mile. Basic features of the radio controller include the two flight mode options, a failsafe switch, and a flight timer. The video monitor provides telemetry and a measured voltage output of the battery. During test flights, the live video feed supplemented line of sight operations within a short distance, but consistent signal loss was experienced beyond about 500 feet. A second video link antenna was installed on the video monitor, in order to improve signal quality. The video link functioned reasonably well up to about 1,250 feet with the additional, more receptive antenna.

During all operations, the flight timer was set at 16 minutes - a value determined based on the expected battery life. A 22,000 milliamp-hour, Tattu lithium-polymer battery (22.2 Volts, 25C, 6S) was used as a power source. The battery was purchased specifically for its AS150 connectors, which are designed for use with the S1000+. It weighs 5.53 pounds and is rated for over 20 minutes of flight time by its manufacturer. The timer was reduced below the rated time to compensate for the added weight of the gas monitor and the large operational area. The S1000+ was landed before the timer ended, if the battery dropped below 20.7 Volts when the machine was not under load.

The failsafe feature was used effectively as an auto-land feature during test flights but was not used during NO<sub>x</sub> sampling. The failsafe was considered as an emergency safety option at the mine sites. It was only to be used in the event that the operator lost sight with the S1000+ for an extended period of time, or if adverse conditions required an immediate landing. An auto failsafe also came pre-programmed into the S1000+, so that the machine would return in the event of a lost link with the radio controller.

The gas monitor attachment selected for use was Industrial Scientific's iBrid MX6 aspirator model. The MX6 is a complex sampling tool that is relatively simple to operate. It is a continuous gas monitor that draws in gas at a nominal rate of 0.3 liters per minute. Pump speed is automatically adjusted by the device, based on inflow resistance. Figure 4.5 shows the MX6. The aspirator inlet protrudes from the upper left corner.



Figure 4.5: iBrid MX6 Gas Monitor, Aspirator Model (Industrial Scientific)

Up to five sensors can function simultaneously, providing a comprehensive view of the local atmosphere. Table 4.1 lists the sensors that were installed during sampling.

Table 4.1: Sensors Installed During Sampling

SENSOR	MEASUREMENT RANGE	RESOLUTION	SENSOR TYPE
Oxygen (O <sub>2</sub> )	0 - 30% Vol	0.1%	Electrochemical
Carbon Dioxide (CO <sub>2</sub> )	0 - 5% Vol	0.01%	Infrared
Carbon Monoxide (CO)	0 - 1,500 ppm	1.0	Electrochemical
Nitrogen Dioxide (NO <sub>2</sub> )	0 - 150 ppm	0.1	Electrochemical
Nitric Oxide (NO)	1 - 1,000 ppm	1.0	Electrochemical

The MX6 is equipped with a data logger, which evaluates gas readings at a user-specified sampling interval and stores the information within internal memory. Data logger entries include various parameters, such as the gas reading, STEL, TWA, a time stamp, and alarm conditions flagged. Throughout this experiment, the interval was set at one second, in order to capture immediate changes in gas concentrations.

Industrial Scientific considers the MX6 to be a lifesaving device. As such, calibration is recommended monthly and bump tests are suggested before each use. A bump test is a controlled procedure where each sensor's target gas is introduced at a concentration just high enough to activate the alarm. Bump tests are intended to verify the correct response of the device before use, so that hazardous atmospheres are properly identified to the user.

Calibration of the MX6 was completed by Industrial Scientific within seventeen days of sampling. The NO sensor was also replaced. Bump tests were not performed in the field for two reasons. First and foremost, bump tests are important when an individual must rely on the gas monitor for protection. Since no human exposure to harmful atmospheres occurred during testing, bump tests were not viewed as a necessity. Secondly, three tanks of specific gas mixtures were required for bump testing. Two of these tanks were not in stock, and transporting the tanks cross-country would have required excessive effort.

The MX6 aspirator model was chosen specifically to avoid rotor downwash during flight. The S1000+ generates violent thrust, even when hovering. As a result, air from above is forced downward, potentially diluting NO<sub>2</sub>, which is heavier than air and is initially expected to be present in larger concentrations lower to the ground. The aspirator can be

used with tubing in order to draw an air sample from an alternate location. Overcoming some influence of downwash was possible by suspending tubing below the S1000+.

Up to 100 feet of 1/8 inch (internal diameter) PVC tubing can be used with the MX6 aspirator model; however, tubing length was limited for use with the S1000+. Tubing naturally coiled and was weighted near the suspended end to maximize length and eliminate recoil. Though only a small amount of weight was necessary to properly control the tubing, longer segments substantially increased stress on the S1000+ because of the moment created. Tubing was taped to the left landing gear leg and foot to prevent it from being stripped from the aspirator in flight. The S1000+ self-corrected to the added external force, but concern arose for potential damage to the landing gear. As a result, tubing was reduced to a reasonable length of 9.33 feet. A 0.75 pound bag of metal weights was taped firmly to the tubing about six inches from the suspended end with enough strength to hold the bag, but not enough to compromise the integrity of the tubing. The gas monitor was placed on the battery tray and secured using a small, 3D-printed mount with one screw. The screw was inserted into the back of the MX6 where the belt clip is normally located. Zip ties were included as an additional safeguard (see Figure 4.13).

Figure 4.6 shows the fully equipped S1000+ from the front. The gas monitor is located below the collapsed, white antenna in the photo. The battery was repositioned on the tray to counter-balance the 1.125 pound gas monitor, so that the center of gravity was located at the center of the S1000+.

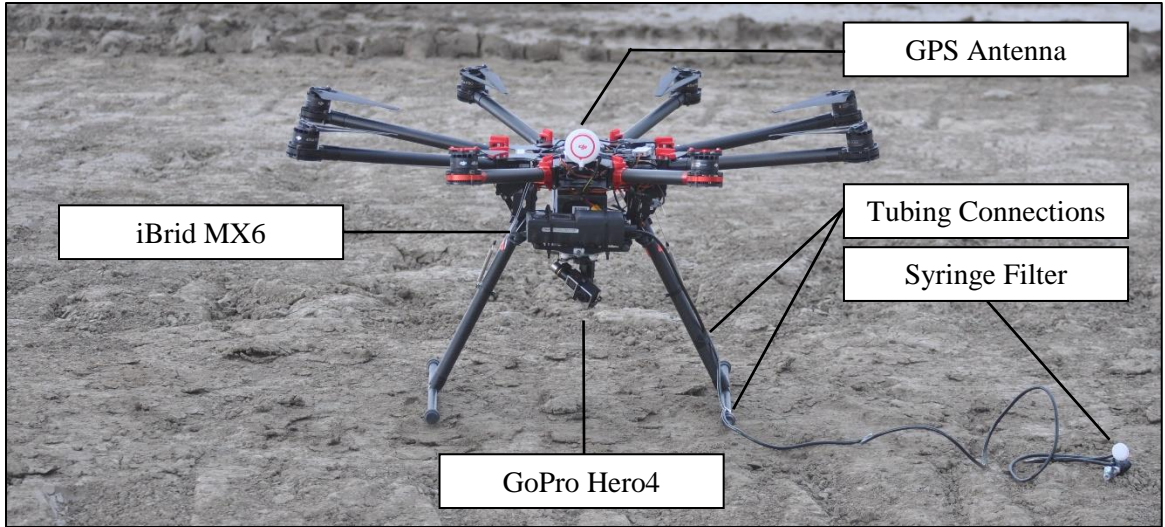


Figure 4.6: Fully Equipped S1000+ (Front View)

The PVC tubing is visible in the lower right of Figure 4.6. A Pall 0.45  $\mu\text{m}$  acrodisk syringe filter was installed at the end of the tubing. Industrial Scientific recommends this filter for dust and moisture collection. A second filter is pre-installed at the aspirator/tubing connection. Industrial Scientific states that a two-second delay in gas measurement is present for every foot of tubing connected to the aspirator. Since 9.33 feet of tubing was used, a delay of 19 seconds was assumed present in all samples.

The GoPro is positioned at an angle in Figure 4.6. The gimbal auto-leveled upon activation, and the operator retained complete control over the vertical angle of the camera in flight. Blasting was also documented from the ground, using a tripod-mounted HD video camera and a handheld, high-resolution Nikon digital camera. Two people were needed to properly document the blasts and operate the S1000+.

### 4.3 Methodology, Flight A

Flight A occurred at Arch Coal's *Black Thunder Coal Mine* near Wright, Wyoming. Prior to Flight A, gas sampling had not been attempted; however, the S1000+ was previously flown with the gas monitor and tubing installed. The observed blast encompassed two benches. A total of 12 holes detonated 23,900 pounds of a 50/50 ANFO/emulsion blend in the upper bench. A total of 99 holes in the lower bench shot 121,650 pounds of emulsion. Figure 4.7 illustrates the outcome. The S1000+ is on approach in the image.



Figure 4.7: Flight A Blast-generated Cloud

It is evident from Figure 4.7 that the cloud on the upper bench shows signs of  $\text{NO}_x$  (pale yellow hue) while the cloud along the lower bench does not. The color difference between the two clouds agrees with what researchers have discovered regarding the relative volume

of NO<sub>x</sub> generated by a 50/50 blend versus pure emulsion (Figure 2.4). The upper cloud was classified as *fume level 1A*. Figure 4.8 illustrates a plan view perspective of the flight.

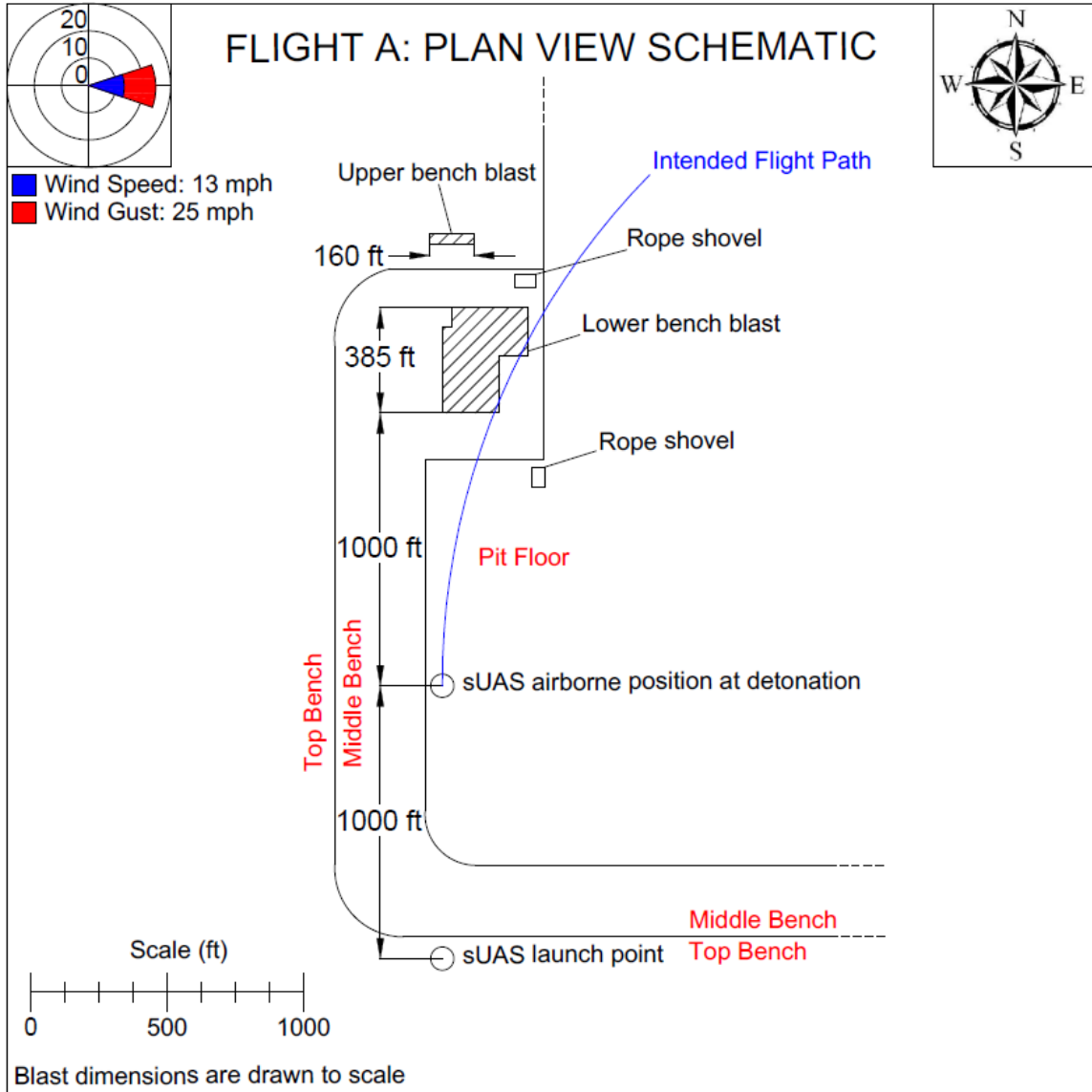


Figure 4.8: Flight A Schematic

The S1000+ was operated from approximately 2,000 feet away, and the operator viewed the flight directly from behind. At this distance, the operator was unable to determine if the S1000+ intercepted the cloud. The coordinates provided by the video monitor were unable to supplement the operator, since the distance to the shot was only an estimate.

Additionally, the wind direction forced the clouds away from the operator. Upon evaluating the results two days later, the data logger showed no measureable concentrations of NO, NO<sub>2</sub>, or CO. It was determined that the operator had a clear understanding of the right and left movement of the S1000+, while the forward and reverse directions were completely indistinguishable. Proposed alterations to the sampling methodology are presented in Chapter Nine.

Prior to takeoff, the control area was selected because of its reasonable view of the blast. In addition, rain had saturated the area, and tire tracks in the mud eliminated most level launch points. A safe perimeter from people and equipment (e.g. pickup trucks and light plants) was established. The wind speed was a steady 13 miles per hour with gusts over 20 miles per hour. Weather approached mission abort conditions (see Table A1 in the Appendix), but the flight was able to be completed safely near the time of the shot. Preparation of the equipment was swift. Once the pre-flight checklist was completed, the gas monitor was activated and a new data log was initiated using the menu on the MX6. The S1000+ was launched six minutes before the blast.

The operator positioned the S1000+ about halfway between the observation area and the lower bench blast. Consistent effort was required to assist the self-correction of the S1000+ in the midst of wind gusts. At detonation, the throttle was maximized to intercept and pursue the emissions with haste. Figure 4.9 displays the operator's reaction to the blast.



Figure 4.9: Full Throttle Acceleration of S1000+

Bringing the S1000+ to a complete stop after achieving peak acceleration required discretion. The suspended tubing tended to swing upward near the rotors. With an abrupt stop, the tubing may have contacted the blades and impaired or eliminated flight capability – potentially knocking the S1000+ out of the sky and destroying it. The S1000+ is capable of flight with only seven of its eight rotors functioning, but this advertised feature was never tested. The throttle was slowly reduced when nearing the desired hover point downrange, allowing the tubing to sway in a relatively calm manner.

#### **4.4 Methodology, Flight B**

Flight B occurred at Arch Coal's *Coal Creek Mine (CCM)*, near Wright, Wyoming. A moderately orange cloud was observed, which was classified as *fume level 3B*. The blast

consumed 330,232 pounds of bulk blasting agent (both 50/50 and 40/60 ANFO/emulsion; ANFO contained 4.167% fuel oil). A total of 328 holes were drilled, but only 267 holes were loaded due to an underlying stream channel that created voids and weakened the local rock mass. The overall powder factor was 0.32 lbs/BCY. Holes were wet, and the sleep time of some loaded explosives was six weeks. Both the poor geologic conditions and lengthy exposure of explosives to water likely exacerbated NO<sub>x</sub> formation. Tables A2, A4, and A5, located in the Appendix, provide additional blast design and weather information. Figure 4.10 shows the blast-generated cloud, which was a mixture of yellow and orange.



Figure 4.10: Flight B Blast-generated Cloud, 30 Seconds Post-blast

It was unanimously agreed among the observers that the blast shot well for the given conditions. The blast was not designed to cast overburden. As a result, the muck remained near its in situ position. Coloration of the air was not visible from the ground observation area for 15 seconds, after which cloud formation was rapid.

The cloud remained low to the ground along the bench; however, it quickly lifted in the direction of the wind. Figure 4.10 displays NO<sub>x</sub> emissions 30 seconds following the blast. The distinct orange color can be seen permeating from the crest of the bench. Figure 4.11 reveals the continuous secretion of NO<sub>x</sub> from the bench face nearly two minutes post-blast. Coloration in the cloud faded from orange to yellow to pale yellow, dispersing completely after about five minutes.



Figure 4.11: Flight B Bench Face Emissions

The operator and assistant improved the documentation of pre-flight procedures during Flight B. Figure 4.12 shows the S1000+ and HD video camera at the launch point, which was approximately 1,000 feet from the nearest row of holes in the blasting pattern.



Figure 4.12: Flight B Launch Point

Figure 4.12 was photographed facing due south. The blasting pattern was 82 holes deep into the image (2,132 feet) and four rows wide (184 feet). Wind was blowing at a consistent 11 miles per hour southeast. A flight area of 2,500 feet in all directions was free of obstructions. The closest object was a dragline boom, which protruded above the spoil, 2,500 feet north of the launch point. Conditions were ideal for flying.

A safe perimeter from people, nearby pickup trucks, and the blaster's truck was established. The S1000+ was set up two hours before the flight and a thorough diagnostic check was completed. It was discovered that one of the arms was loose at its connection with the S1000+ frame, presumably from the combined abuse during shipment cross-country and the heavy forces experienced during Flight A. The arm was repaired before takeoff.

At the 10 minute blast warning, the gas monitor was powered on and a new data log was started. Figure 4.13 shows the gas monitor attachment on the battery tray.



Figure 4.13: Flight B Gas Monitor Activation

The time on the gas monitor was announced while the HD video camera was recording, at which point the time on the camera was also stated verbally. These times were later used in conjunction with file creation times and common events in the photos/videos to correlate cloud coloration with gas concentration data points.

Before the one minute warning, the S1000+ was energized by connecting the battery terminals. Energization only activated the GPS – the rotors were not turning. Just after the one minute warning, the rotors were activated and takeoff was initiated. Figure 4.14 displays the S1000+ hovering briefly above the launch point.

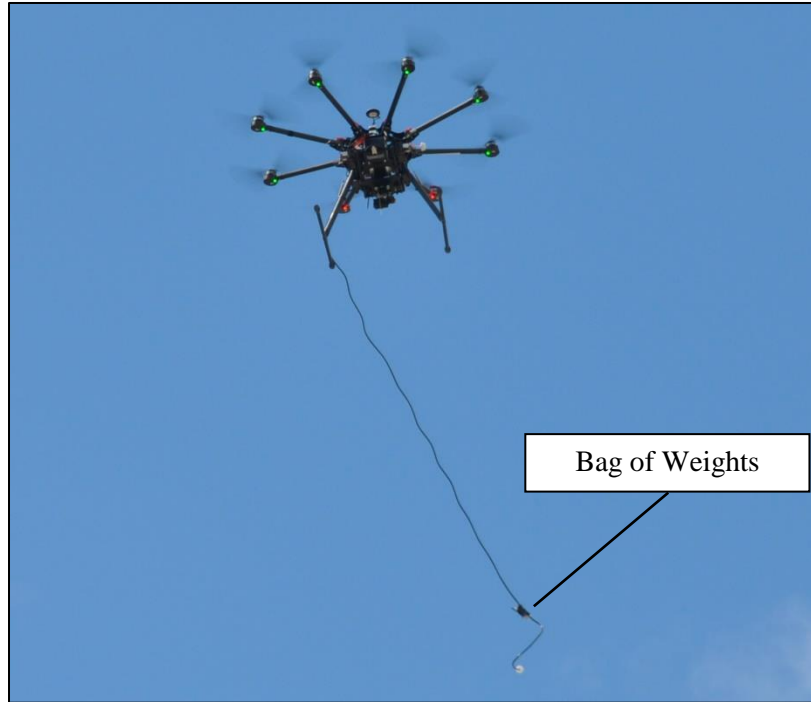


Figure 4.14: S1000+ Hovering with Suspended Tubing

Figure 4.14 provides a useful perspective of the PVC tubing. The S1000+ can be seen hovering with a slight leftward pitch as the tubing sways toward the right, illustrating the effect of the weighted tubing with only minor movement. The bag of weights is visible near the suspended end of the tubing. There was not excessive concern for flight failure because of the tubing, since the rotors provided such a substantial amount of thrust. The operator was proficient at protecting the S1000+, as well. Overall, the observation presented in Figure 4.14 indicates that smaller sUAS may not be suitable for use with suspended tubing.

At detonation, the S1000+ was airborne at approximately 500 feet from the closest row of holes. The throttle was raised to its maximum position immediately. Limited hesitation was required to avoid fly material, and the operator intercepted the cloud in seconds. Figures 4.15 and 4.16 illustrate the progression of the blast and the flight schematic, respectively.



Figure 4.15: Flight B Blast Sequence

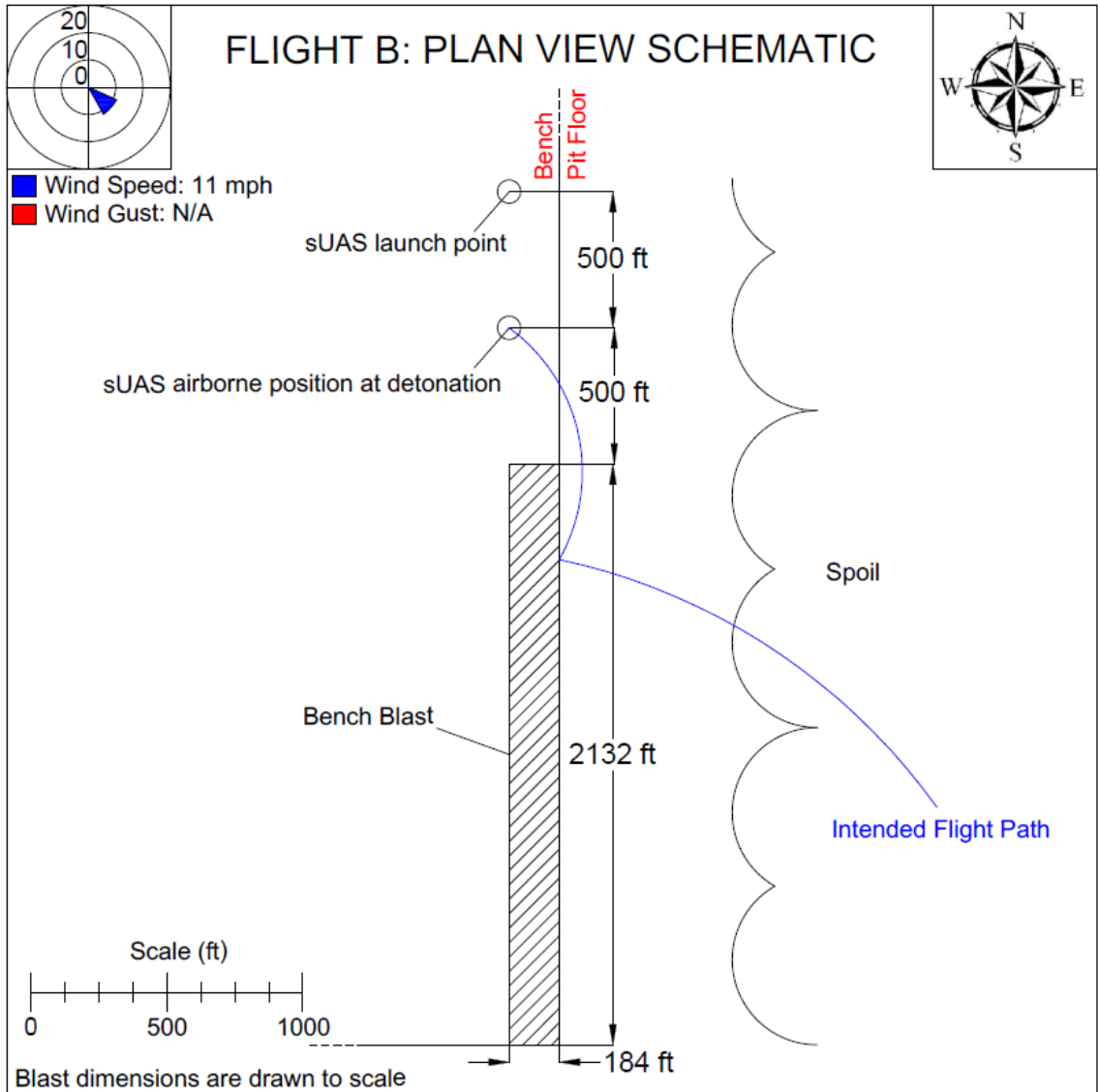


Figure 4.16: Flight B Schematic

Figure 4.16 reveals the reduced proximity between the operator and the blast (compared to Flight A). It was planned to intercept the cloud as it formed and then position the S1000+ at a stationary point downwind.

As previously mentioned, the S1000+ is capable of two flight modes: course lock and home lock. With course lock active, the S1000+ flies along a rectangular grid, based on the forward position at takeoff and regardless of its rotational orientation. Alternatively, home lock forces the S1000+ to move about the launch (home) point, also regardless of its orientation. Figures 4.17 and 4.18 illustrate the flight modes.

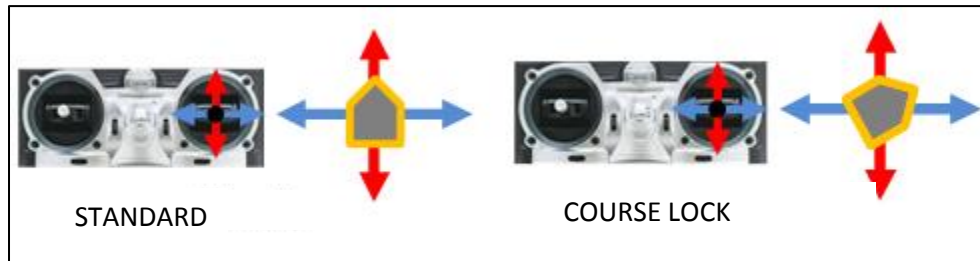


Figure 4.17: Course Lock Flight Behavior (DJI Wiki, Intelligent Orientation Control)

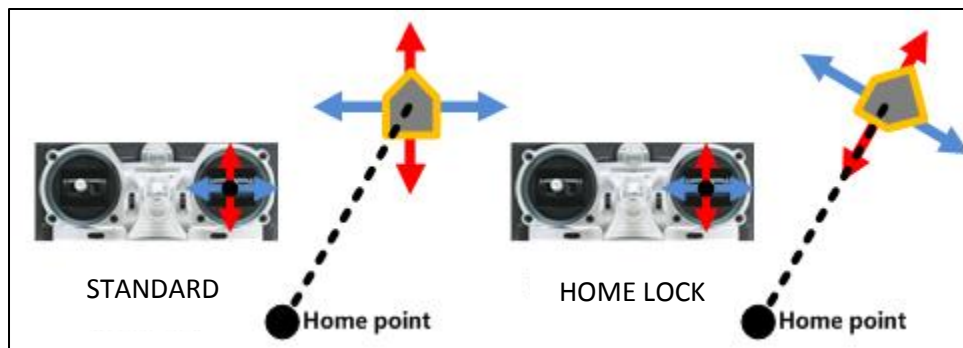


Figure 4.18: Course Lock Flight Behavior (DJI Wiki, Intelligent Orientation Control)

The operator experimented with both modes during Flight B. Initially, the S1000+ was placed in course lock, since the control area was oriented directly in line with the blasting pattern and nearly perpendicular to the wind direction (i.e. a square flight pattern was

expected to function efficiently). The use of course lock on takeoff provided excellent control of the S1000+ at close range and at first contact with the blast-generated cloud.

After sampling the initial toxicity from the cloud, the operator attempted to track the cloud using home lock. Home lock's radial turning control allowed the operator to align the S1000+ with the downwind direction and begin pursuing the cloud in a straight line. Unfortunately, the operator suffered from depth perception issues, similar to Flight A. The most valuable information was collected early near the bench. Downwind toxicities were captured inadequately.

It was determined from the flight mode evaluation that course lock is most useful when the operator is aligned perpendicular to the wind direction. In addition, course lock becomes difficult to use at long distances, since movements of the S1000+ are directionally indistinguishable. Home lock is advantageous downrange, since the operator can move toward and away from the launch point with certainty.

Flight B was six minutes and fifty-five seconds in duration. The S1000+ was landed manually approximately 10 feet from the launch point. The operator was cautious on descent to prevent the tubing from catching the rotors near the ground. When the S1000+ was approximately five feet above the ground, the operator added thrust and nudged it in the direction of the right landing gear, so that the tubing spread out gently. Figure 4.19 shows the S1000+ just after power down with the tubing at its side.



Figure 4.19: Flight B Landing

Once landed, the gas monitor was powered off. A post-flight examination of the S1000+ showed no signs of stress, so the arms and antenna were collapsed. Results were evaluated once the gas monitor was docked at a computer.

#### **4.5 Sampling Results, Flight B**

The blast-generated cloud was intercepted by the S1000+ three seconds after coloration was observed from the control area, or 18 seconds after detonation. A sample of the cloud was collected from the darkest orange region, displayed in Figure 4.10. Using file creation times generated by the various devices, common events in the photos and videos, and the time stamps provided by the gas monitor, the gas concentration measurements were correlated with still frames extracted from the GoPro flight camera. Figures 4.20 and 4.21 therefore illustrate a relationship between cloud color and  $\text{NO}_x$  concentration.

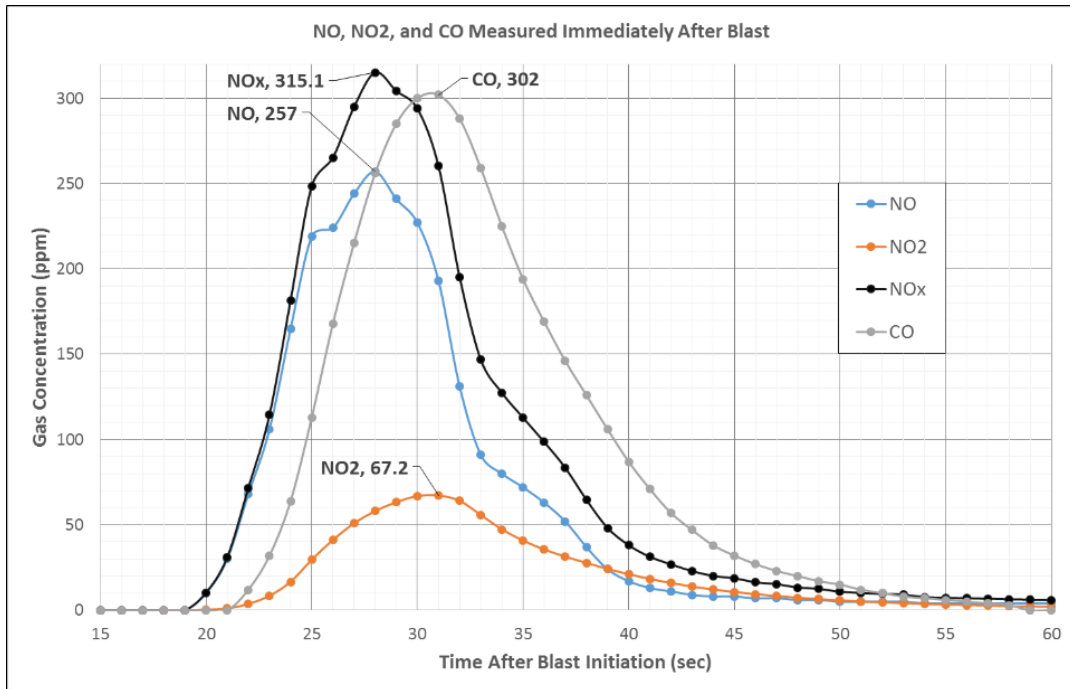


Figure 4.20: Immediate NO<sub>x</sub> and CO Concentrations

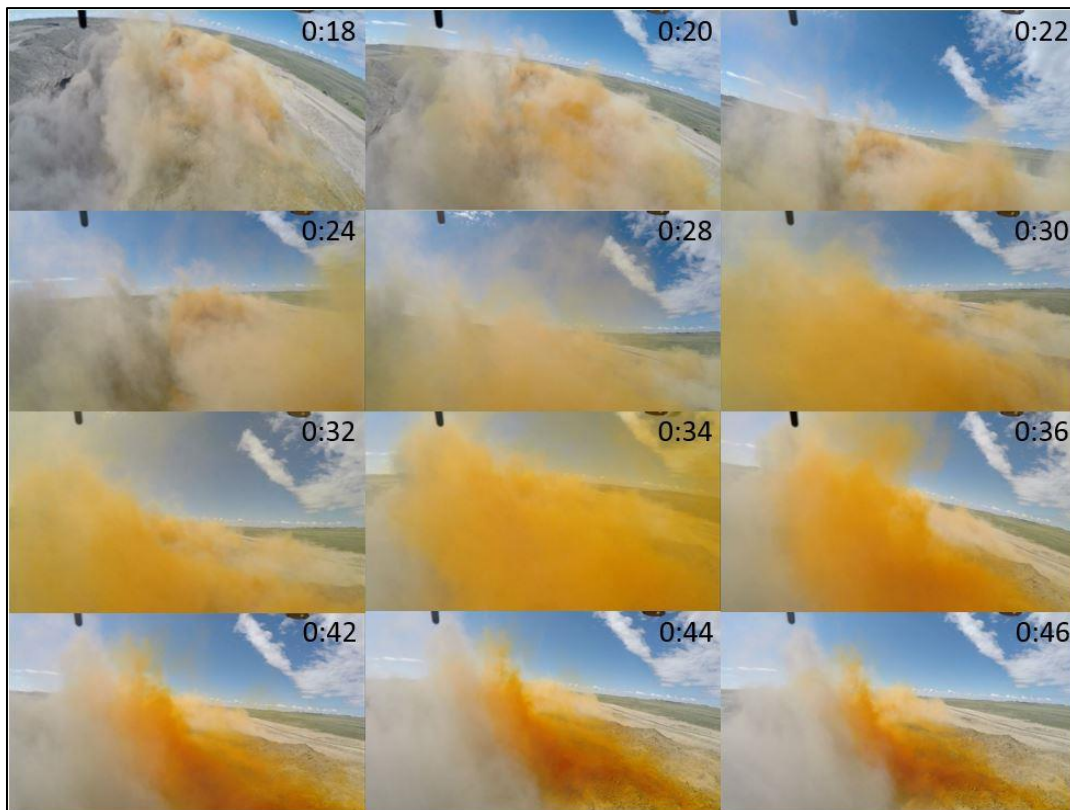


Figure 4.21: GoPro Video Frame Sequence

The sequence of images displayed in 4.21 was created using the flight camera. From 0:18 to 0:22, the S1000+ was accelerating into the cloud. Between 0:22 and 0:34, the S1000+ was stationary, hovering over the crest of the bench. After 0:34, the S1000+ was removed from the cloud to identify the coloration of the measured sample (the PVC tubing was suspended 7.6 feet below the landing gear; therefore, the sampled orange color is not visible in images before 0:42).

The data presented in Figure 4.20 reveal the immediate impact on the local atmosphere. The peak NO and NO<sub>2</sub> measurements (257 ppm and 67.2 ppm, respectively) are believed to be the ceiling concentrations representative of the observed blast. The decline in the readings following 0:34 is caused by the movement of the S1000+ out of the cloud and in opposition to the wind. Dissipation of the cloud is not a contributing factor. The portion of the decline occurring before 0:34 is suspected to be the result of a wind gust undercutting the PVC tubing inlet.

An estimate of the total volume of NO<sub>x</sub> produced by the blast was calculated from the ranges presented in Figure 2.4. Approximately 149,791 kilograms (330,232 lb) of bulk agent were detonated. A 50/50 blend was used to represent the outcome, since holes were loaded with either a 50/50 or 40/60 ANFO/emulsion blend. A range of 5.0 L/kg to 31.0 L/kg yielded an estimated total NO<sub>x</sub> emission between 748,954 liters and 4,643,518 liters.

## Chapter Five: Additional Sampling

### 5.1 Overview

A third flight was conducted at a surface mine in the United States. The event is referred to as Flight C. The circumstances of Flight C were different than the two flights previously described. A summary is provided below:

- A blast-generated cloud was observed from a distance of 15,000 feet. The cloud was dark red to brown, indicative of very high  $\text{NO}_x$  concentrations. The S1000+ was positioned directly downwind and launched to a ceiling of 400 feet. Gas samples were collected, in order to evaluate detectable NO and  $\text{NO}_2$  concentrations.

Instrumentation used for sampling was unchanged, though this cloud was not documented with the tripod-mounted HD video camera.

### 5.2 Methodology, Flight C

Figure 5.1 shows the immediate aftermath of the blast. The dark red and brown colors indicate  $\text{NO}_x$  concentrations in excess of the gas readings collected during Flight B.



Figure 5.1: Flight C Blast-generated Cloud

The cloud was classified as *fume level 5C*, which is the most severe designation and describes the worst-case local atmospheric impact. Though no data representative of the colors shown in Figure 5.1 were collected, the cloud's dispersion was closely monitored at from a distance of approximately 15,000 feet. Figure 5.2 displays the flight schematic. The blasting pattern dimensions and distance to the permit boundary are estimates.

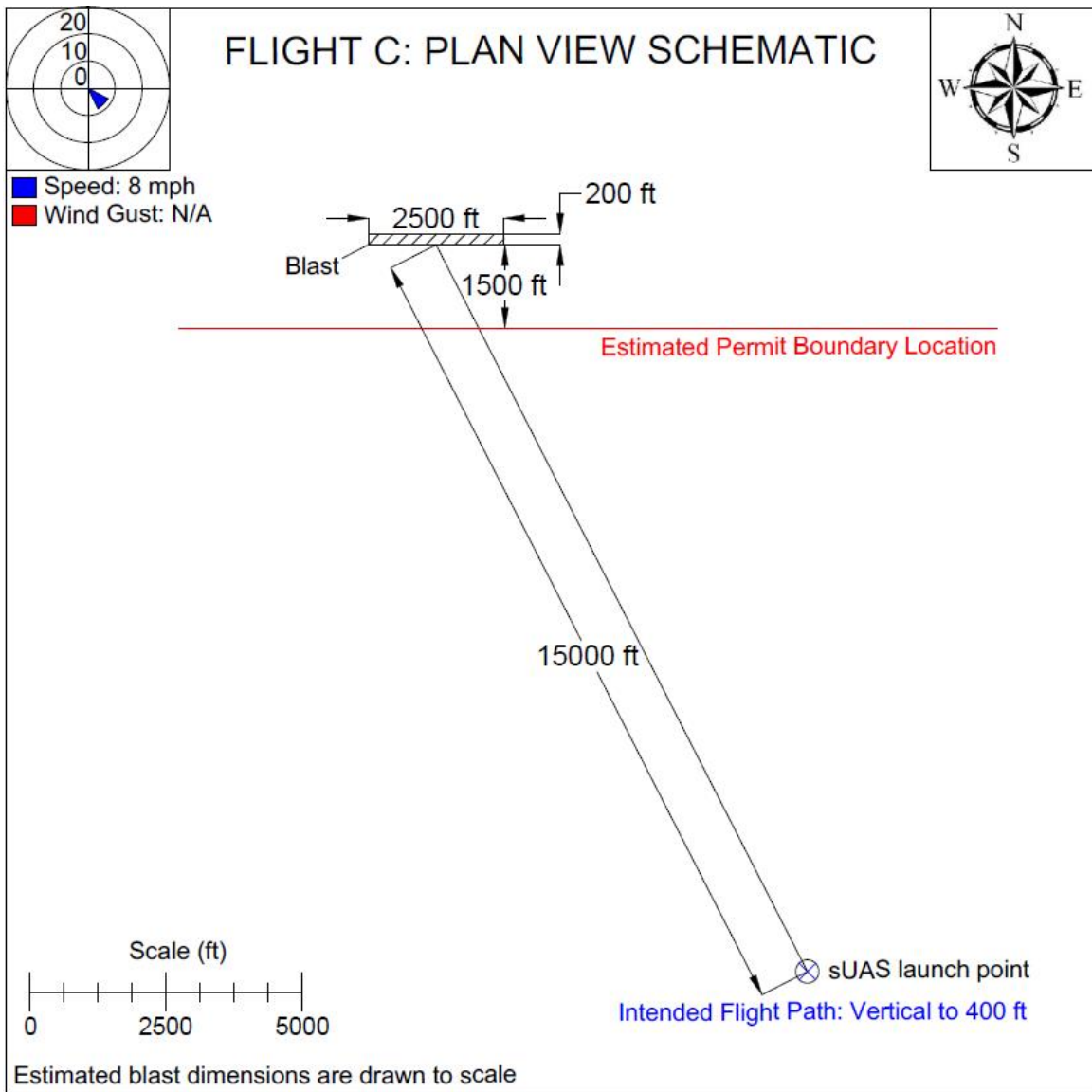


Figure 5.2: Flight C Schematic

The wind direction transported the cloud directly toward the control area. As the cloud passed directly overhead, the S1000+ was launched to 400 feet (the maximum ceiling permitted by the FAA for the University of Kentucky's sUAS research). Figure 5.3 shows the coloration in the sky at launch.



Figure 5.3: Flight C Blast-generated Cloud Overhead

It was observed during flight that the visible yellow hue overhead, indicative of an  $\text{NO}_2$  concentration above 2.5 ppm, was higher than the 400 foot ceiling – though this was speculation until the quantitative results were evaluated later. It was not possible to determine where the visibly-toxic concentrations began and ended in the vertical direction.

### 5.3 Sampling Results, Flight C

The graph presented in Figure 5.4 illustrates NO<sub>2</sub> readings measured between activation of the S1000+ and its descent to the ground.

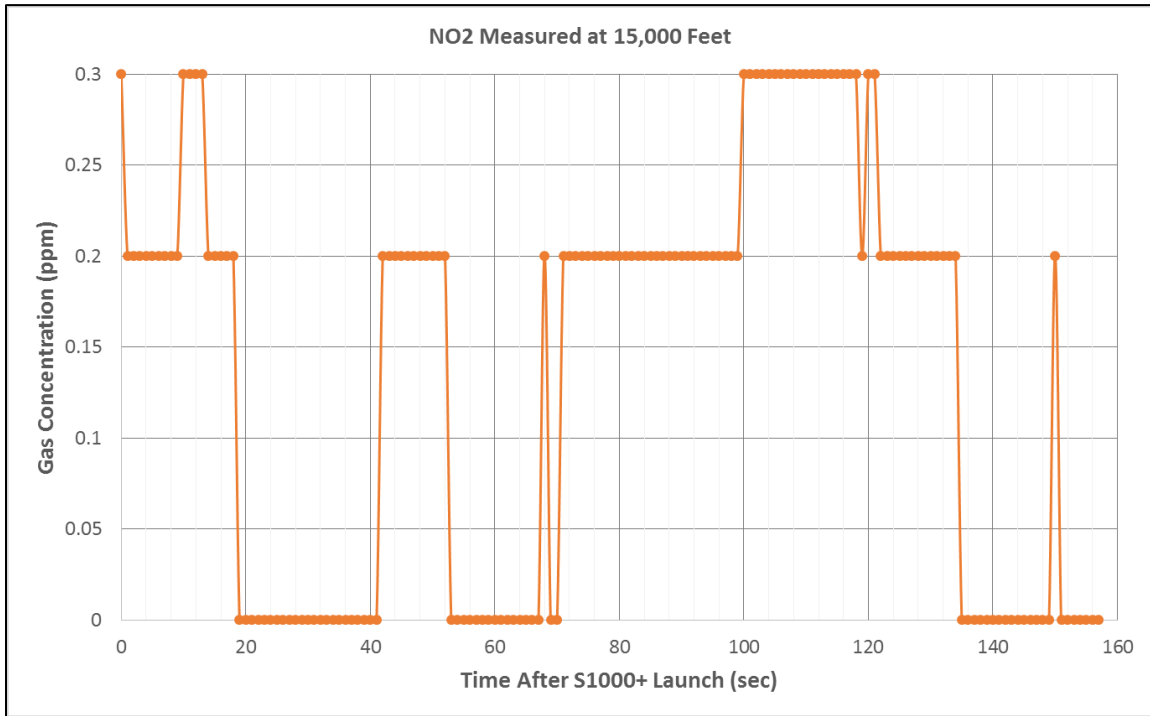


Figure 5.4: NO<sub>2</sub> Measurements 15,000 Feet Downwind

Concentrations of NO<sub>2</sub> up to 0.3 ppm were measured in the space between ground level and 400 feet. A pungent scent was noticeable at the observation area, typical of blasting. The odor threshold of NO<sub>2</sub> is 0.12 ppm, though it is uncertain if NO<sub>2</sub> was the cause. Other gases not measured by the monitor may have also been present (e.g. ammonia). It was also observed from the gas monitor data that NO and CO were absent from the local atmosphere. Lack of NO suggests complete oxidation of the unstable gas to NO<sub>2</sub>. Since the yellow coloration in the sky was observed above the flight ceiling (verified by NO<sub>2</sub> measurements consistently below 2.5 ppm), it is suspected that a substantial amount of the NO originally

present inside the cloud was lifted by the wind (since NO is lighter than air) and later oxidized to NO<sub>2</sub>. Overall, these results demonstrate that even the most severe NO<sub>x</sub> emissions from surface blasting are capable of dissipating to minor concentrations at ground level less than three miles from their origin, given the appropriate weather conditions (Table A3). Cloud dispersion is discussed further in Chapter Six.

## **Chapter Six: Blast-generated Cloud Dispersion**

### **6.1 Overview**

The instantaneous peak toxicity of blast-generated NO<sub>x</sub> must be considered in a broader context before risk to human health and safety can be fully evaluated. Dispersion of blast-generated clouds is an additional factor requiring evaluation. Dispersion is affected by an assortment of variables. Wind speed, initial cloud toxicity, scale of the emission, and total volume of NO<sub>x</sub> produced are generally considered to be the most important. The following two sections review the cloud dispersion during Flights B and C, respectively.

### **6.2 Cloud Dispersion Results, Flight B**

Originally, it was planned to position the S1000+ downwind of the blast in a stationary location to monitor declining NO<sub>x</sub> concentrations over time; however, poor depth perception at the lengthy operating distance hindered the ability to gather useful readings, since the operator was constantly attempting to determine the position of the S1000+ relative to the cloud. The video monitor attached to the radio controller was not able to supplement the operator, since the transmission was almost entirely diluted by distance. As a result, intermittent gas concentration measurements from the periphery of the cloud were collected. Figure 6.1 displays the readings captured after the initial 60 second post-detonation sampling window. An additional 355 seconds were logged before the gas monitor was powered off (5.9 minutes), but no gases after registered above zero after 155 seconds (since the sUAS was removed from the cloud unintentionally and eventually returned for landing); therefore, the horizontal axis in Figure 6.1 terminates at this time.

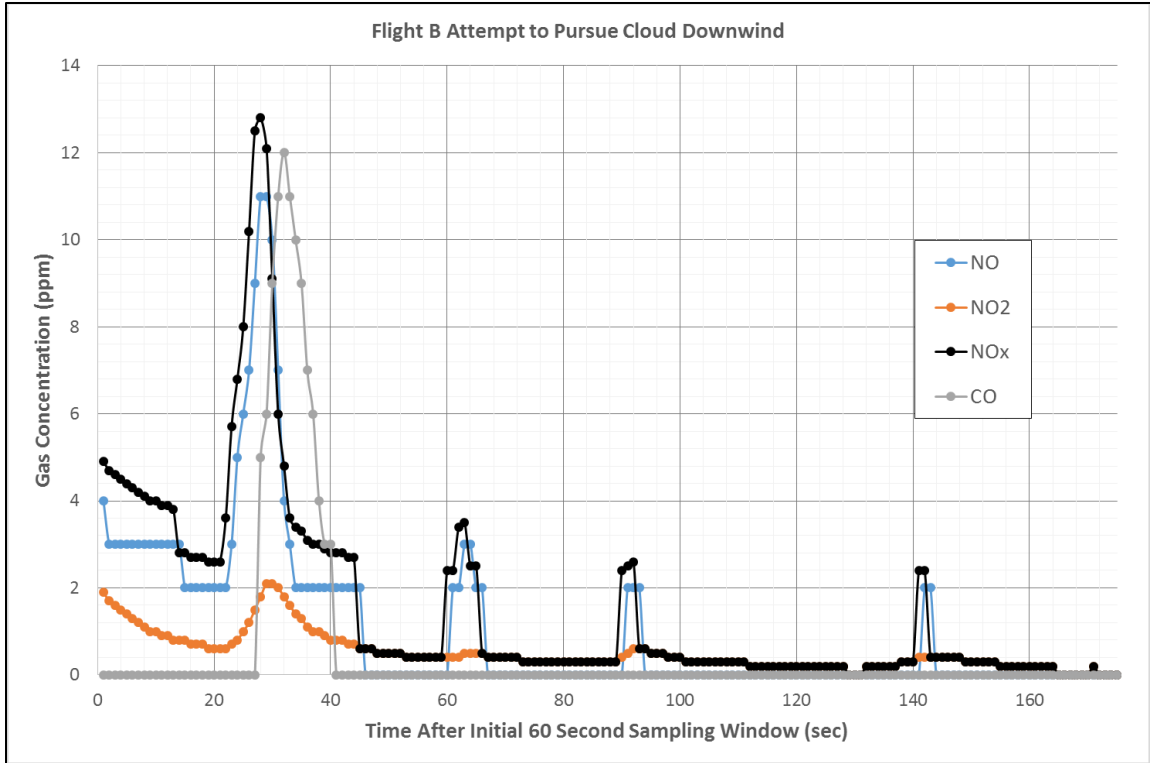


Figure 6.1: Sampling Near Cloud Periphery in Downwind Direction

Figure 6.1 shows four distinct spikes in gas measurements, which resulted from slight penetration of the S1000+ into the cloud. It is estimated that the dispersion data presented in the graph were collected between 250 and 1,250 feet downwind from the blast origin. The gas concentrations appear to follow an inverse relationship with time, but the results do not provide a definitive dispersion rate, since the position of the S1000+ was not constant. Future dispersion sampling should be conducted at stationary distance intervals.

While quantitative dispersion sampling was not immediately useful, behavior of the cloud was monitored efficiently from the control area. Figure 6.2 illustrates the rapid dispersion in a sequence of images, captured with a high-resolution digital camera. The camera zoom and photo angle are not consistent, since the camera was held in hand. In addition, images later in the sequence place more emphasis downwind.

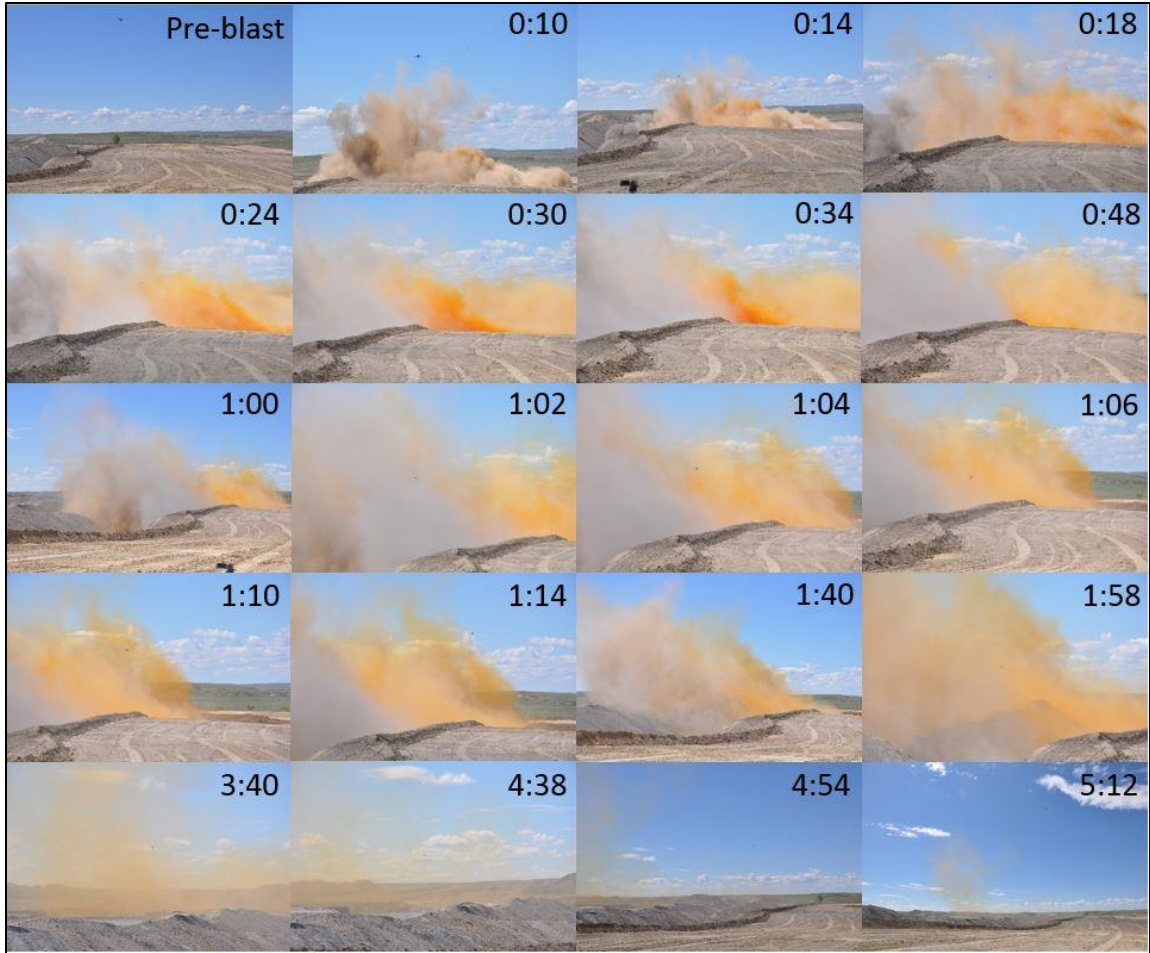


Figure 6.2: Flight B Dispersion Image Sequence

Figure 6.2 shows fading coloration as the gases and dust lift. The dark orange color disappears in a matter of 30 seconds. After approximately five minutes, no visibly-toxic concentrations of  $\text{NO}_2$  are present. A small amount of dust was aroused by the wind several minutes after the blast but the air remained free of obvious  $\text{NO}_2$  presence.

A simple geometric dispersion model was developed, in order to calculate the unit volume of  $\text{NO}_x$  generated (i.e. per kilogram of explosive detonated) for comparison with previous lab research (Figure 2.4). Physical observations were used to construct the model. For example, the cloud generated by the blast at CCM lifted at 45 degrees in the direction of

the wind (Figure 4.11). Additionally, coloration disappeared after about five minutes, indicating an NO<sub>2</sub> presence of at most 2.5 ppm. Relevant assumptions are listed below, and an explanation of the mathematical procedure is provided following Figure 6.3.

- Gases and air were mixed evenly throughout a right isosceles wedge
- The distance of the wedge's base was defined by the wind speed and the time until all coloration disappeared (05:12, mm:ss)
- The total volume of NO<sub>x</sub> produced was represented by a 50/50 blend of ANFO and emulsion, as discussed in Section 4.5
- All NO in the dispersion zone had fully oxidized into NO<sub>2</sub> (thus, the volume range of NO<sub>x</sub> produced is referred to as the volume of NO<sub>2</sub>)
- The volume of the blast zone wedge was defined by the pattern dimensions (184 feet by 2,132 feet) and is included in the dispersion zone volume
- The volume of NO<sub>2</sub> in the blast zone was calculated using the peak toxicity of 67.2 ppm and was not the total volume released (see volume range in Figure 6.3)

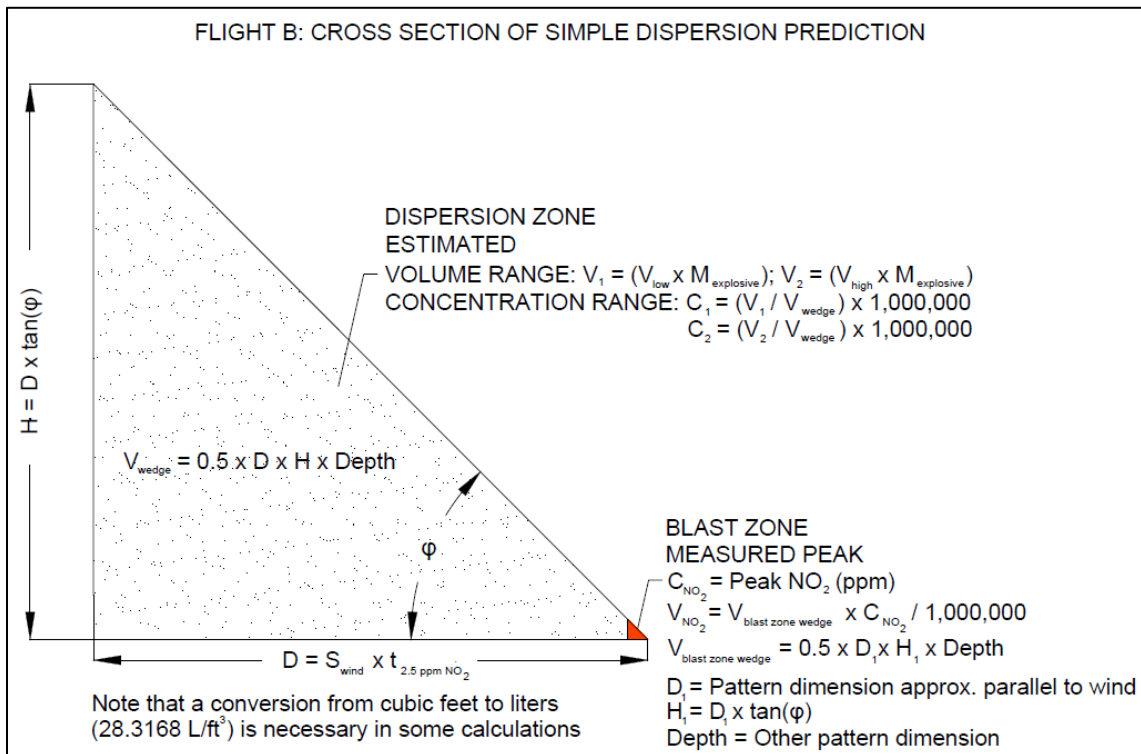


Figure 6.3: Flight B Geometric Dispersion Model

The blast zone is largely informational. It is formed using the pattern dimensions, cloud lift angle ( $\varphi$ ), and peak concentration of  $\text{NO}_2$  measured. The volume of  $\text{NO}_2$  in the blast zone is the instantaneous volume during the peak measurement – if that peak is evenly distributed within the blast zone wedge; however, it does not represent the total volume of  $\text{NO}_2$  emitted by the blast, since more of the gas permeates from the muck for a short time.

The larger dispersion zone wedge includes the blast zone and is the only feature of the model that is necessary to calculate the unit volume of  $\text{NO}_x$  generated. Its base is constructed using the visible threshold of  $\text{NO}_2$ . In other words, the variable  $D$  is the maximum distance that the gases in the wedge can be carried by the wind by the time coloration fades completely ( $\text{NO}_2 \approx 2.5$  ppm). The wedge's height is defined in the same geometric manner as the blast zone, except the value of  $D$  is used instead of the selected blasting pattern dimension,  $D_1$ .

The volume range of  $\text{NO}_2$  within the dispersion zone is derived from previous lab research and is used to validate whether or not the value of  $D$  is reasonable.  $V_{\text{low}}$  and  $V_{\text{high}}$  are the smallest and largest unit volumes of  $\text{NO}_x$  produced by a particular explosive product, measured in liters per kilogram (Figure 2.4). The variable  $M_{\text{explosive}}$  is the mass in kilograms of the blasting agent detonated. Assuming that all  $\text{NO}$  is oxidized to  $\text{NO}_2$  during the time used to calculate  $D$ , the products of  $V_{\text{low}}$  and  $V_{\text{high}}$  with  $M_{\text{explosive}}$  provide a range of possible  $\text{NO}_2$  volume ( $V_1 - V_2$ ) within the dispersion zone wedge. The volume range can be converted to a concentration range ( $C_1 - C_2$ ) in parts per million, using ratios with the total volume of the dispersion zone. If an  $\text{NO}_2$  concentration of 2.5 ppm falls within the concentration range, then the value of  $D$  (thus the dispersion zone geometry) is acceptable.

The unit volume of NO<sub>x</sub> is determined by the known NO<sub>2</sub> concentration of 2.5 ppm and a reorganized version of the ratio used to convert V<sub>1</sub> and V<sub>2</sub> to C<sub>1</sub> and C<sub>2</sub>. The unit volume can be described as NO<sub>x</sub> instead of NO<sub>2</sub>, because NO oxidizes to NO<sub>2</sub> by a 1:1 molar relationship (Equation 1, Section 2.3). Equation 2 below shows the method of unit volume calculation.

$$V_{unit} = \frac{2.5 \text{ ppm } NO_2}{1,000,000 \text{ ppm}} * V_{wedge} \quad (2)$$

Figure 6.4 illustrates the results of the calculations presented in Figure 6.3. The same model schematic is used.

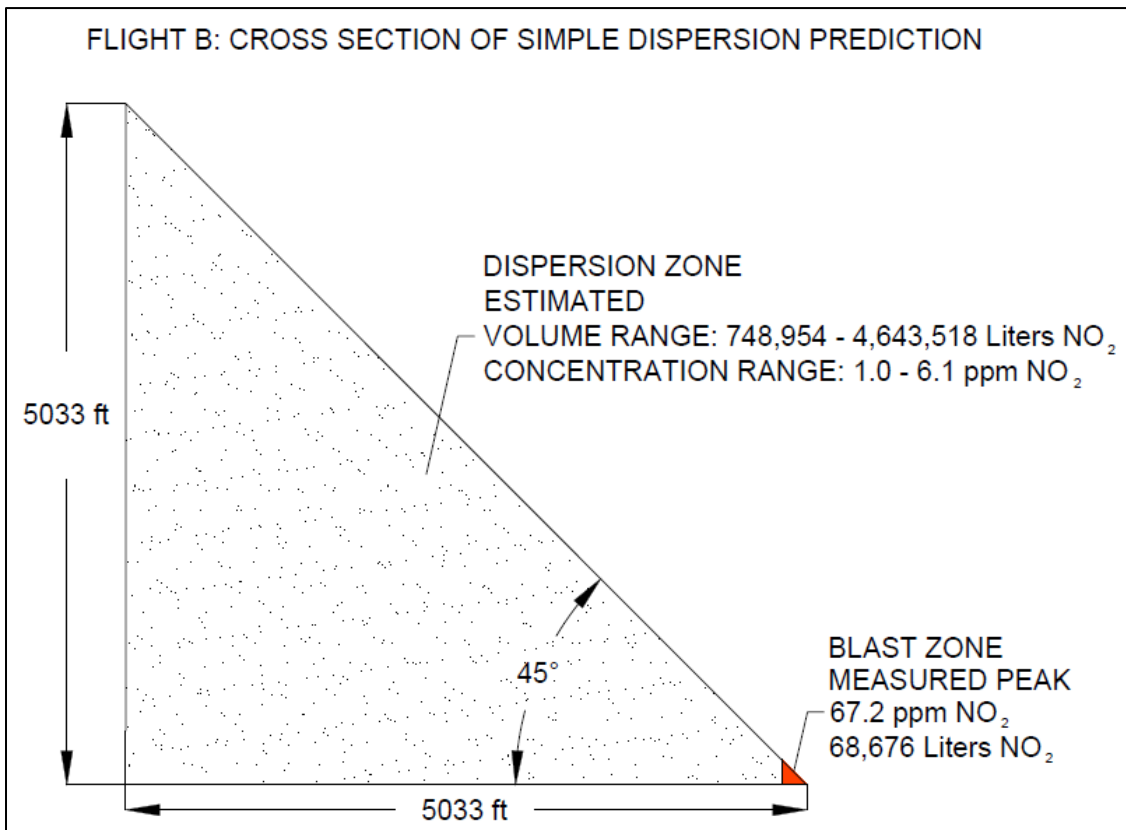


Figure 6.4: Flight B Geometric Dispersion of NO<sub>x</sub>

Calculations suggest that the NO<sub>2</sub> concentration in the dispersion zone was 1.0 to 6.1 ppm. Since the wedge volume was developed using the distance the cloud traveled until visible NO<sub>2</sub> disappeared (NO<sub>2</sub> ≈ 2.5 ppm), the dispersion zone geometry is valid. Calculation of the unit volume indicates that approximately 12.8 L/kg of NO<sub>x</sub> were generated for every kilogram of 50/50 blend detonated.

Figure 6.5 is an updated version of Figure 2.4 that includes the estimated unit volume of NO<sub>x</sub> generated by the blast at CCM (listed as “McCray, 2016” for a 50/50 blend).

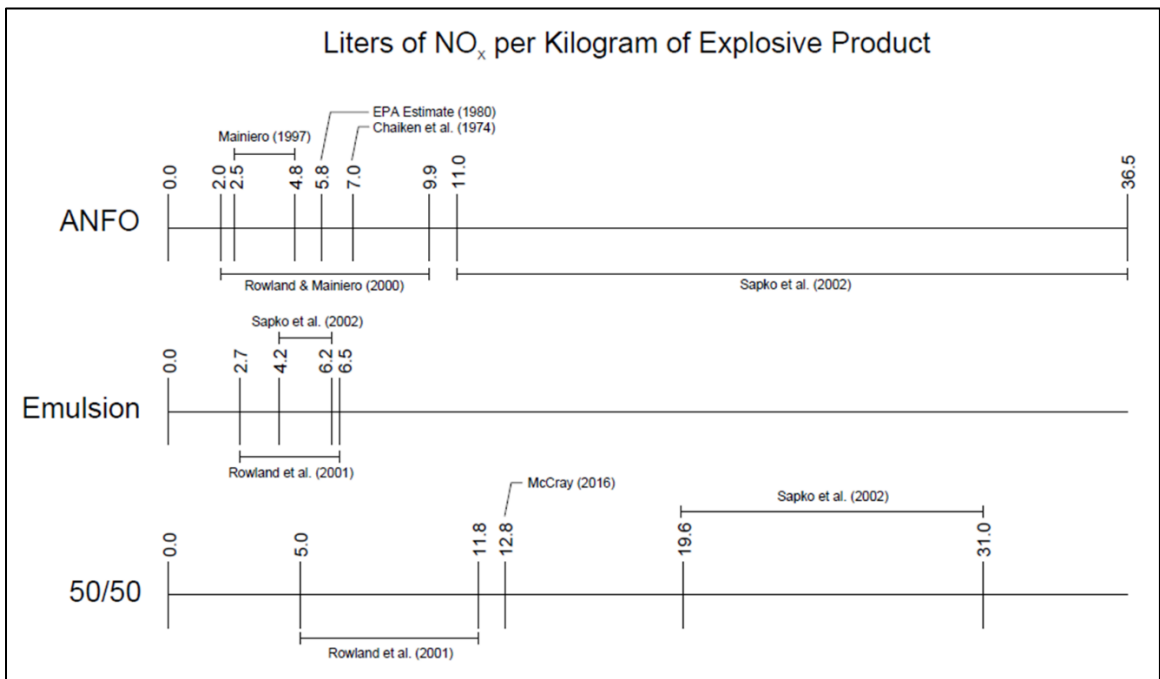


Figure 6.5: Relevant Estimates of Blast-generated NO<sub>x</sub> Updated

The simple dispersion model is useful because it is derived from physical observations. While a number of assumptions are necessary to develop the model completely, it can be validated to some extent by lab data. Judgment of the cloud lift angle and instant when coloration disappeared are subjective but can be overcome using a sensitivity analysis (i.e. varying  $D$  and  $\varphi$  to develop a range of unit volumes instead of a point estimate).

### 6.3 Cloud Dispersion Results, Flight C

A similar geometric modelling technique was applied to the Flight C measurements; however, the calculations were carried out with a different purpose. Since no blast zone measurements were recorded, the goal of the Flight C model was to back calculate an estimate of the *initial NO<sub>2</sub> concentration* using data collected downwind. The following assumptions were applied to the model:

- Nearly identical weather conditions on the Flight B and Flight C observation days permitted the use of a right isosceles wedge, even though the true cloud lift angle was not visible from the observation area
- Gases and air were mixed evenly throughout the right isosceles wedge
- The distance of the wedge's base was defined by an approximate 15,000 foot distance between the blast and the observation area
- All NO in the dispersion zones had fully oxidized into NO<sub>2</sub> (thus, the volume of NO<sub>x</sub> produced is referred to as the volume of NO<sub>2</sub>)
- The volume of the blast zone wedge was defined by estimated pattern dimensions, since no shot report was obtained (200 feet by 2,500 feet)
- The volume of NO<sub>2</sub> in the blast zone was assumed to be the summation of both dispersion zones (a value likely larger than reality)
- The volume of NO<sub>2</sub> in the ground level dispersion zone was calculated using an evenly-distributed peak of 0.3 ppm measured below an altitude of 400 feet
- The volume of NO<sub>2</sub> in the above ground level dispersion zone was determined using an evenly-distributed 2.5 ppm NO<sub>2</sub> (since a pale yellow color was visible in the sky) and does not include the volume of the ground level dispersion zone

Figure 6.6 demonstrates the mathematical procedure necessary to fully develop the model.

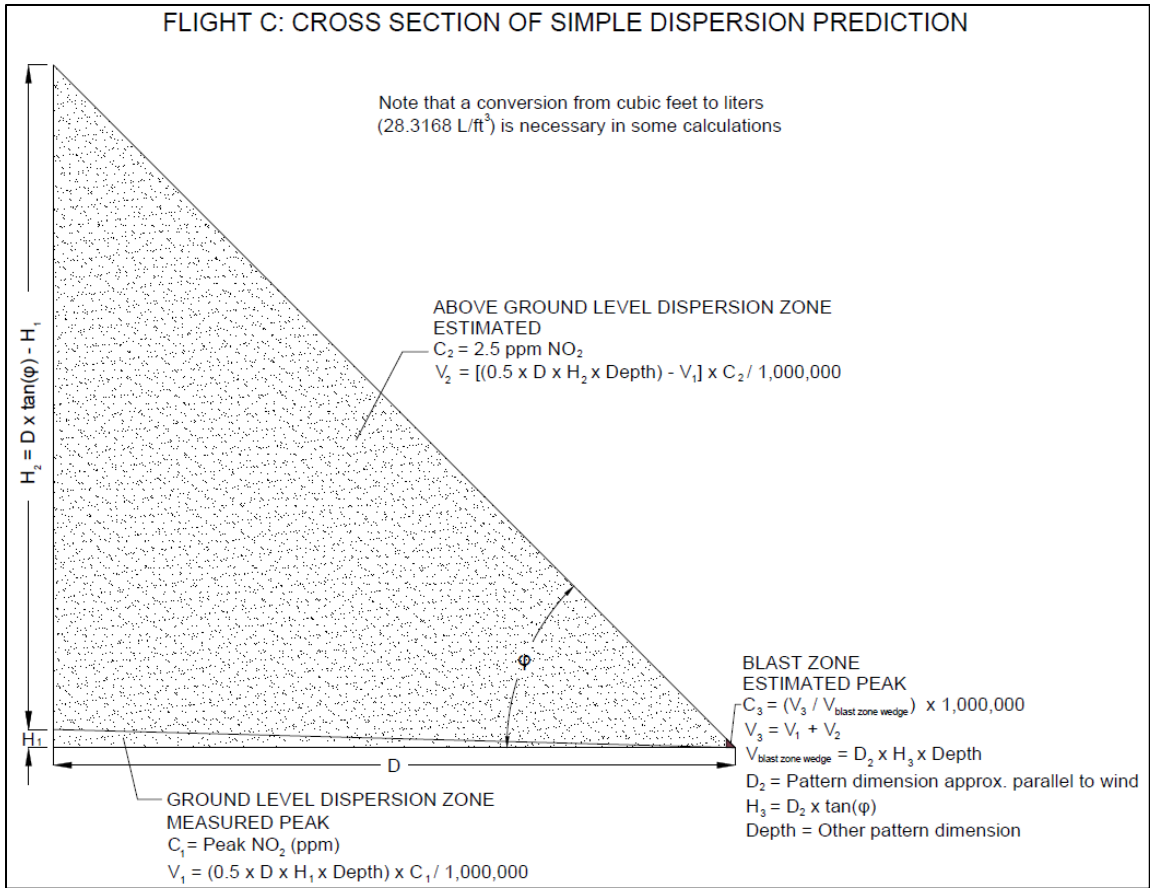


Figure 6.6: Flight C Geometric Dispersion Model

Samples were collected at a known distance,  $D$ , from the blast origin, and below the flight ceiling,  $H_1$ . If it is assumed that the peak NO<sub>2</sub> was evenly-distributed within the ground-level dispersion zone, then a volume of NO<sub>2</sub>,  $V_1$ , can be determined.

The above-ground-level dispersion zone is defined using the same distance,  $D$ , and the cloud lift angle,  $\phi$ . The volume of the above-ground-level dispersion zone does not include the volume of the ground-level dispersion zone. Coloration was observed above 400 feet; therefore, an NO<sub>2</sub> concentration of 2.5 ppm is assumed to be the average within the above-ground-level dispersion zone. Calculation of volume  $V_2$  provides an estimate of NO<sub>2</sub> within the above-ground-level dispersion zone.

The summation of  $V_1$  and  $V_2$  is an estimate of the total  $\text{NO}_2$  generated by the blast. If this total volume was present instantaneously within the blast zone (defined by the pattern dimensions and cloud lift angle), then the peak concentration of  $\text{NO}_2$  present within the initial blast-generated cloud,  $C_3$ , can be calculated. Figure 6.7 shows the analysis outcomes.

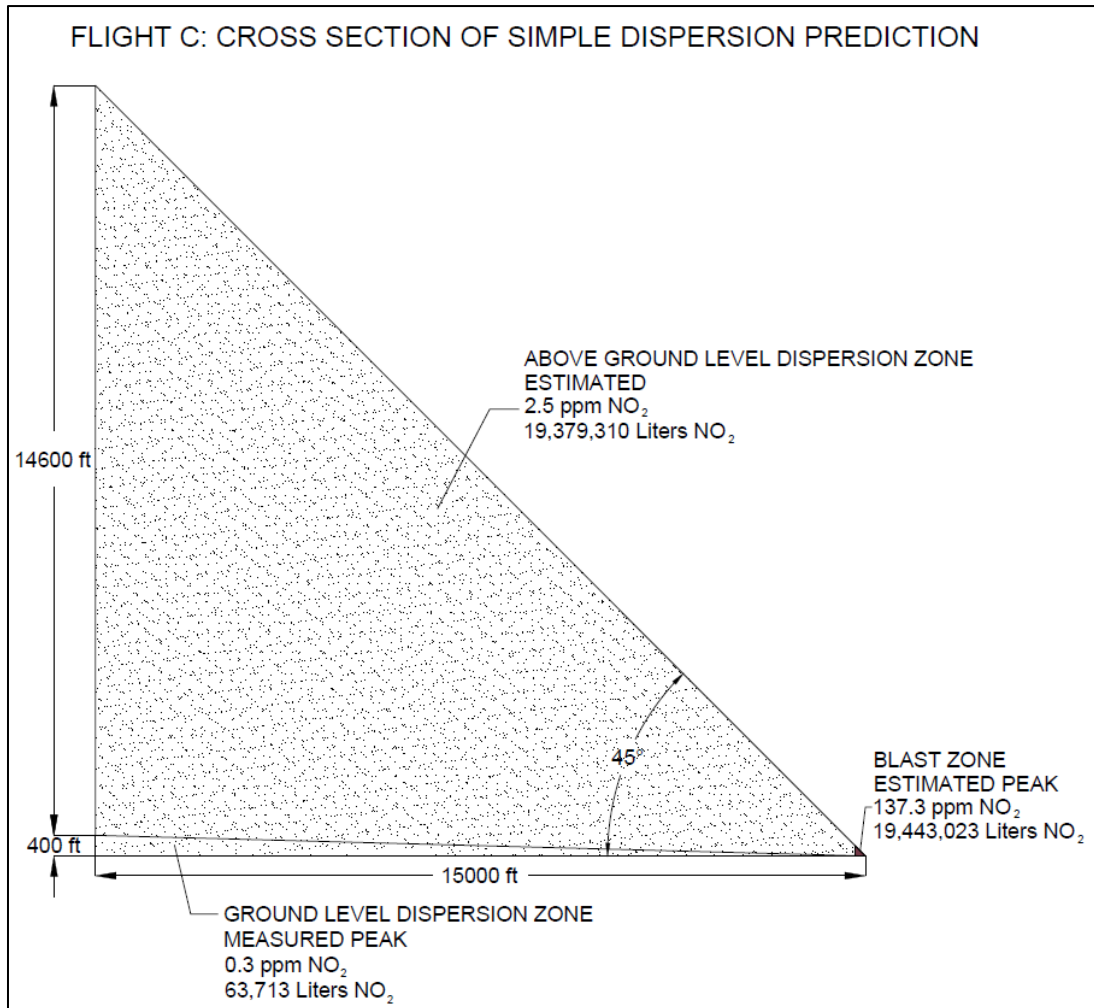


Figure 6.7: Flight C Geometric Dispersion of  $\text{NO}_x$

The results presented in Figure 6.7 provide an estimate of 137.3 ppm  $\text{NO}_2$  in the blast zone. The calculated value is larger than the 67.2 ppm peak measured during Flight B and is therefore agreeable with the relative colors of the clouds. It is also more indicative of a  $\text{NO}_2$  emission than total  $\text{NO}_x$ , since the  $\text{NO}_x$  concentration during Flight B peaked at 315.1

ppm – much higher than 137.2 ppm. The shot report was not obtained for this blast but would have greatly improved the informational value of this model, since a range of NO<sub>x</sub> volume generated at the blast zone could then be calculated. In addition, the wedge dimensions could be modified, based on the true blasting pattern dimensions.

While 137.2 ppm NO<sub>2</sub> is a highly toxic concentration of the gas, the dispersion of the cloud over a short distance provides useful evidence that even intense emissions of NO<sub>x</sub> from surface mine blasting are only immediately concentrated for a small amount of time. Dispersion in varying wind speeds should be evaluated to form a comprehensive understanding of *fume level 5C* toxicity. In addition, the assumption that air is evenly mixed is a challenging burden to overcome in this simple model. Realistically, NO<sub>2</sub> is heavier than air and is likely to reside lower in the dispersion zone; however, the measurement of 0.3 ppm below 400 feet with coloration in higher regions of the sky (i.e. > 2.5 ppm) demonstrates the general lift of the cloud, given the appropriate weather conditions.

## **Chapter Seven: Health Implications**

### **7.1 Overview**

It is understood that visible concentrations of NO<sub>2</sub> are indicative of unhealthy atmospheres; however, the human health and safety impact of surface mine blasting emissions requires additional context. Risk to mine workers and the public is a function of initial cloud toxicity, scale of blasting, and cloud dispersion behavior. Defining these factors qualitatively does not adequately identify risk. Direct samples from the two large blasts offer an initial, quantitative perspective of blast-generated NO<sub>x</sub> in a full-scale mining environment, which heretofore has remained virtually absent from the body of scientific knowledge. The sample size of this experiment is too small to form a comprehensive conclusion, but the available data and observations show that there is little concern for human exposure to hazardous levels of NO<sub>2</sub> if the appropriate precautions are taken.

Studies cited by OSHA and NIOSH largely focus on exposure to minor concentrations of NO<sub>2</sub> for extended periods of time; however, abrupt exposures to elevated concentrations of NO<sub>2</sub> provide the most relevant comparisons to blast-generated NO<sub>2</sub>. For this reason, the NIOSH IDLH value offers the best description of immediate health concern for mine employees. Other existing standards, such as the OSHA ceiling PEL and EPA NAAQS, are most applicable to the public, which may infrequently come into contact with a diluted concentration of the emitted NO<sub>2</sub>.

## 7.2 Mine Employee Health

Instantaneous ceiling concentrations of NO and NO<sub>2</sub> measured during Flight B were 2.57 and 3.36 times greater than the associated NIOSH IDLH values, respectively. These levels were detected in the blast zone (i.e. in the immediate vicinity of the detonation). Additionally, it is estimated that the ceiling concentration of NO<sub>2</sub> within the Flight C blast zone was 6.87 times greater than the IDLH. Although the initial NO and NO<sub>2</sub> exceeded life-threatening concentrations, the gases are not likely to cause harm in the normal course of mining – if mines prone to regular and/or substantial emissions of NO<sub>x</sub> consider both the sources of NO<sub>x</sub> and the previously discussed dispersion variables during the development of *blast(ing) area* perimeters.

According to the Mine Safety and Health Administration (MSHA), *blasting area* is defined for surface coal mines to be “the area near blasting operations in which concussion or flying material can reasonably be expected to cause injury” (30 CFR § 77.2, 1999). MSHA defines a more comprehensive *blast area* for surface metal/non-metal mines as “the area near the blasting operations in which concussion (shock wave), flying material, or gases from an explosion may cause injury to persons.” The blaster in charge is responsible for the development of a blast area and must consider the following factors to protect individuals from such hazardous blasting outcomes (30 CFR § 56.2, 2004):

- Geology or material to be blasted
- Blast pattern
- Burden, depth, diameter, and angle of the holes
- Blasting experience of the mine
- Delay system, powder factor, and pounds per delay
- Type and amount of explosive material
- Type and amount of stemming

While establishing safeguards against blast-generated gases is mentioned in the definition of blast area, this practice is not explicitly stated in the list of factors; however, it can be inferred that mines with an emission history of NO<sub>x</sub> are responsible for developing a blast area based on such previous experiences. For this reason, the causes of NO<sub>x</sub> – particularly exposure of explosives to water and sleep time – should be considered during delineation of blast area perimeters. In addition, the scale of the blast, wind speed, and wind direction are also pertinent factors.

A common rule of thumb for the blast area perimeter is 1,000 feet from the nearest row of holes in all directions. Individuals must not enter the area (and are prevented from doing so) before the shot is fired and the blaster in charge approves of the outcome. The rule of thumb is based on fly material, which is unlikely to be ejected with enough energy to travel beyond a few hundred feet. While the preliminary NO<sub>x</sub> sampling and dispersion observations presented in this document suggest that highly-toxic NO<sub>x</sub> concentrations are short-lived, expanding the blast area perimeter to create a broader *blast area exclusion zone* – with emphasis downwind – is in the best interest of mine employees.

Table 2.2 (pg. 12) provides an example of a blast area exclusion zone method. Downwind distances were defined using dispersion modelling software, which considered initial toxicity of NO<sub>2</sub>, several wind speeds, and a fixed emission volume. Similar tabulated tools can be attuned on a site-by-site basis by (1) creating detailed, in-house case histories using direct sUAS sampling or (2) drawing from a larger body of knowledge in the near future once NO<sub>2</sub> concentrations can be further attributed to explosive sleep time, scale of blasting, and other relevant sources of the gas. In either case, seasonal weather differences at individual mines will be paramount in forecasting the necessary exclusion zone.

At this time, mines with regular NO<sub>x</sub> emissions are generally aware of the gases but may not have strategies in place to provide provisional protection for workers. Until the health risk is fully quantified by additional sampling studies, mines should (1) withdraw all workers, without exception, to a position beyond the current rule of thumb definition of blast area, (2) remove workers farther downwind from the blast area, based on the total weight of explosives to be detonated and the sleep time of the explosives (i.e. experience with previous NO<sub>x</sub> emissions), and (3) blast with elevated caution in low wind speeds. Table 2.2 shows that slower air movement requires an extended exclusion zone; therefore, wind speeds below about 5 miles per hour indicate that workers should be removed from an extended downwind distance. It has been observed that mines in the United States often observe the opposite behavior; they do not wish to blast during elevated wind conditions, especially if the direction is not favorable (i.e. toward a nearby town). Greater wind speeds are believed to improve dispersion and should be examined during future studies.

There are two additional NO<sub>x</sub> hazards that should be noted. The first is defined by weather (wind speed and direction) and the second is avoidable with minimal effort.

1. NO<sub>2</sub> is denser than air, and the gas may be retained in the pit below a bench blast. For this reason, equipment operators and other mine personnel may come into contact with the gas if natural ventilation is unable to effectively dilute it. These individuals should take caution when returning to work, even after the blast is cleared. In addition, those observing the blast from the pit should also be cautious of rapid cloud formation. If the wind does not lift or remove the cloud, hazardous levels of NO<sub>2</sub> may be confined within the pit and propagate elsewhere.

2. Equipment operators are not necessarily removed from the blast area and often remain inside their machines within the 1,000 foot rule of thumb blast area perimeter. Figure 4.7 shows two manned hydraulic shovels within this perimeter after detonation of the blast during Flight A. The shovel beyond the white smoke is positioned downwind. If operators remain near overburden blasts in this manner, NO<sub>2</sub> exposure may occur. Cab filters are not designed to eliminate toxic components from the atmosphere, and cabs intended to recirculate clean air are not perfectly insulated. As such, removal of operators from the area is prudent.

By introducing a more detailed delineation of blast area perimeters, it is likely that mine workers will remain safe from even minor concentrations of NO<sub>2</sub>. Mines should begin documenting NO<sub>x</sub> emissions, including photography of cloud formation and dispersion and recording of weather data. Applying the proposed direct sampling method will advance the development of blast area exclusion zones and solidify the necessary protective measures.

### 7.3 Public Health

A prominent health concern is the transit of elevated NO<sub>2</sub> levels outside of mine permit boundaries. The Environmental Protection Agency's (EPA) has designated 100 ppb (0.1 ppm) as the short-term national ambient air quality standard (NAAQS) for NO<sub>2</sub>. Both the enormity and remoteness of most mining operations offer substantial protection for the public (esp. mines in the Powder River Basin); however, it is possible for large clouds to propagate for some distance. The cloud monitored during Flight C demonstrated arguably the worst-case scenario for NO<sub>x</sub> emissions. Its characteristics are summarized below:

- The cloud was designated as *fume level 5C*, indicating that the NO<sub>2</sub> concentration within the cloud was ranked as the most severe (estimated peak of 137.3 ppm).
- The initial scale of the cloud was immense (estimated to be 2,500 feet across and 200 feet in height/depth).
- The cloud crossed the permit boundary and was measured 15,000 feet away from the blast origin (2.84 miles).
- The gas monitor detected NO<sub>2</sub> concentrations up to 0.3 ppm between the ground and 400 feet, with visibly-toxic concentrations higher in the atmosphere.
- The average NO<sub>2</sub> concentration during the 158 second flight was 0.138 ppm.
- An additional 10 seconds of data before takeoff showed an NO<sub>2</sub> presence between 0.2 and 0.3 ppm. Including these values increases the average NO<sub>2</sub> to 0.147 ppm.

The measurements taken downwind during Flight C are not directly attributable to the hour-long NO<sub>2</sub> average concentration, since the total sampling time was short; however, it can be inferred that the risk of public exposure to harmful concentrations of NO<sub>2</sub> was minimal. It is unlikely over the passage of time that any larger concentration of NO<sub>2</sub> would have been observed, primarily because the measurements were taken at first contact with the gases (i.e. the least amount of dispersion time was provided to the cloud). If the true hour-long average concentration is regarded as either the measured average of 0.147 ppm

or the measured peak of 0.3 ppm, then the applicable EPA AQI designation at 15,000 feet from the blast was “unhealthy for sensitive groups” (Table 2.4). It is believed that that the hour-long NO<sub>2</sub> average was much lower than 0.147 ppm – even within compliance of the NAAQS limit.

Flight C provides useful evidence that the most severe NO<sub>x</sub> emissions are capable of dispersion to low ground-level concentrations over distances of at most 15,000 feet. It is uncertain what concentrations were present between the mine permit boundary and the control area, though no coloration was observed low in the sky due to consistent lifting of the cloud. For these reasons, the preliminary sampling suggests that risk to public health and safety is low.

## **Chapter Eight: Challenges of Utilizing an sUAS for NO<sub>x</sub> Sampling**

### **8.1 Complicated FAA Restrictions**

The FAA finalized its rules for the registration and operation of sUAS in the national airspace on June 21, 2016. Previously, acquiring the necessary documentation to fly for commercial or research purposes (i.e. non-hobbyist activities) involved months, and various restrictions were imposed on the applicant. Complying with some mandated restrictions (such as the need for a licensed pilot) was challenging for many who were seeking to take advantage of sUAS technology. The new rules have not been published for a long enough duration to establish their challenges, but it is expected that the new requirements (e.g. remote pilot certificate with a small UAS rating) will also be complicated to obtain.

Prior to June 21, 2016, commercial sUAS operations required a Certificate of Waiver or Authorization (COA) or Exemption to Section 333 to the FAA Modernization and Reform Act of 2012 (FMRA). Completion of this project was possible through the University of Kentucky (UK), which possessed a blanket area public agency COA for unmanned aerial vehicle flight operations. General restrictions under the UKCOA and other similar FAA approvals included the following:

- Airspace ceiling limit (e.g. 400 feet AGL)
- Daylight operations only
- No operations within five miles of airports
- Line of sight operation
- Notice to airmen (NOTAM) filed with the FAA before each flight

Specific safety procedures, such as protocol for lost link events and low battery conditions, were also required to be clearly stated and understood.

The UKCOA also mandated the presence of two people during any flight event. These individuals were to be medically approved to fly, and at least one was required to hold a valid pilot's license. The greatest challenge affecting the completion of this project was coordination with a licensed pilot.

## **8.2 Weather Limitations**

The application of an sUAS for gas monitoring is limited by weather conditions such as rain and wind. Most sUAS devices capable of sustaining flight with the weight of the suggested gas monitor attachment are large, and sensitive electronic components are often exposed. As such, excessive water exposure may cause irreparable damage. Flying in rain is also dangerous because it is possible that electronics will cease operation in flight and cause the sUAS to fall uncontrollably the ground.

Most manufacturers rate sUAS devices for a specific, maximum wind speed. In some coal-mining regions, the wind is comparably low with the Powder River Basin; however, data collection with this method is currently most relevant to Powder River Basin blasting, due to regularly-visible NO<sub>x</sub> emissions. Wind exceeding 20 miles per hour is likely to force any sUAS to remain grounded.

## **8.3 Seasonal Impact on Gas Monitor Usage**

Similar to weather concerns, seasonal temperature ranges will also affect the functionality of both sUAS devices and gas monitors. Sampling during the winter months may not be

possible. For example, the operating temperature ranges of the S1000+ and MX6 iBrid gas monitor are 23 °F to 140 °F and -4 °F to 131 °F, respectively.

#### **8.4 Gas Monitor Calibration and Upkeep**

The MX6 iBrid and similar gas monitors require regular calibration intervals (e.g. once monthly). There are two methods of calibration available (in most cases). First, the owner can mail the monitor to the manufacturer and pay a fee. Second, the owner may choose to purchase tanks of calibration gases and follow a series of specific steps to calibrate the device manually.

It was elected to mail the MX6 iBrid prior to field sampling in this experiment, since three separate tanks of calibration gas were required to complete the process. Two of the necessary tanks were also not in stock for purchase. Calibration by mail is less convenient, but purchased tanks must be stored properly and are difficult to transport. In addition, the gaseous contents of the tanks degrade over time and are only useful for a maximum of about two years.

Sensors within the gas monitors are additional components that require upkeep. Sensors (such as those for NO and NO<sub>2</sub>) generally last for one to three years and are relatively expensive to replace. Replacement is not permitted by the average gas monitor user, either. The selection of gas monitors capable of measuring NO<sub>x</sub> are considered life-saving devices. For this reason, only the manufacturer and certain qualified personnel are permitted to service the monitors.

## **8.5 Drone Reliability/Maintenance**

Most sUAS components are complex and sensitive. Careful inspections of the technology must occur with regularity in order to preserve functionality. The S1000+ and similar models are large and capable of causing serious damage to people and property. As a result, detailed understanding about the mechanics, capabilities, and maintenance is necessary for proper use. Maintenance may include exchanging rotors, troubleshooting electrical systems using software, and testing various flight systems prior to operation. A serious time commitment is therefore a requirement for sustaining the reliability of an sUAS.

## **8.6 Distraction for Mine Employees**

Individuals are often fascinated by sUAS operations, particularly because of their unique applications. As a result, sUAS devices may become a distraction from other important tasks. Reducing awareness at mine sites has dangerous implications, especially for equipment operators. Maintaining a business-as-usual attitude for those observing is crucial, since a key advantage of the technology is safety. Jeopardizing safety in other areas of the mining operation strips any value that the sUAS provides for gas monitoring.

## **8.7 Encouragement of Poor Decision-making**

Although the application of an sUAS for gas monitoring offers large operating distances – and therefore safety for operators – it is likely that some individuals will be encouraged to approach blast sites for improved visibility. Challenges with depth perception at observation distances of 1,000 feet or greater are certain. Though there are available strategies to overcome these challenges (Section 9.1), poor judgment may increase risk of injury or death from blasting outcomes.

Historically, fly material ejected during detonation has caused many fatalities because of poor communication and/or close human proximity to blasting (Bajpayee et al., 2003). Operators approaching the bench may either not communicate their intentions or come too close. Such behavior is detrimental to the liability of mining companies and security of mine personnel that might choose to join the operator.

## **Chapter Nine: Proposed Alterations to Methodology**

### **9.1 Overcoming Depth Perception Issues**

Depth perception was the single largest issue affecting sUAS-based gas sampling. At long distances downrange, directional movements of the S1000+ became indistinguishable to the operator (particularly forward and reverse). No data were collected during Flight A, since the S1000+ did not intercept the blast-generated cloud. Similarly, dispersion monitoring during Flight B was inhibited, because the S1000+ was unknowingly operated only at the cloud periphery. It is expected that the addition of a spotter and a laser range finder will overcome the negative influence of depth perception on future sampling.

Flights A, B, and C required a team of two individuals to complete. Ultimately, the team concluded that the addition of a third individual would have improved results. Future sampling will include a spotter, who will observe from a position perpendicular to the flight path. Using a handheld radio, the spotter will provide information on the relative forward and reverse movements of the aircraft. It is expected that sampling will receive the greatest benefit from this change to the methodology, since positional suggestions can be announced from an alternate perspective in real time during flight.

The addition of a laser range finder will also positively affect sampling but will require additional planning by the operator prior to takeoff. Previously, the operating distance relative to the blasting pattern was estimated. A laser range finder will be used in the future to identify the downrange location of various landmarks (e.g. the highwall(s), equipment, or light plants) relative to the control area. Positional information, provided by the operator's video monitor, will be compared with the measured distances during flight, to

supplement visual limitations. Range finding will be added to the pre-flight checklist, and the operator will need to apply his or her own judgment to capture the most useful distances.

## **9.2 Improving Sampling**

The samples analyzed by the gas monitor are believed to be accurate and representative of the tested atmospheres; however, sampling can be improved by minor adjustments to the tubing attachment and modifications to the S1000+ standard operating procedures (SOPs).

Currently, the sampling tubing's inlet is suspended 7.60 feet below the landing gear to avoid rotor downwash. It is suspected that the impact of downwash is still present, even at this length. Doubling the tubing will further eliminate sample dilution. The added tubing will also facilitate sampling near the crest of the muck, since the operator will not need to position the S1000+ as closely. As a result, the chance of damage or destruction to equipment will be reduced. Test flights with additional tubing first need to be conducted to evaluate the impact of added tubing on flight characteristics of the S1000+, before attempting this strategy in the field.

In addition to equipment adjustments, data analyses can be enhanced through amendments to the S1000+ SOPs. User error was observed in the gas monitor data collected during Flight C. Industrial Scientific recommends two seconds per foot of tubing. A total of 19 seconds were therefore required to completely clear the tubing attachment. The gas monitor was deactivated shortly after landing and prior to the 19 second recommendation. Consequently, the measured sample was not representative of the full descent from 400 feet (which ultimately did not negatively impact results in this experiment). In the future,

the S1000+ operator must be aware of the sampling delay and should not deactivate the gas monitor immediately after landing. The data logger should remain active for at least the duration necessary to meet Industrial Scientific's sampling timeframe.

## Chapter Ten: Conclusion

Sampling results reveal that the instantaneous peak concentration of NO<sub>2</sub> in moderately-orange, blast-generated clouds can be as high as 67.2 ppm – a value 3.36 times greater than the NIOSH IDLH concentration of 20 ppm. It is estimated that, in extreme cases, the instantaneous peak NO<sub>2</sub> concentration can be as high as 137.3 ppm, which exceeds the IDLH limit by 6.87 times.

Cloud dispersion observations show that it is possible for large, moderately-orange clouds to dissipate in just over five minutes. Severe NO<sub>x</sub> emissions (dark red to brown/purple clouds) require more time to disperse under similar weather conditions. Ground-level NO<sub>2</sub> concentrations (0 to 400 feet vertically) were measured with an sUAS at 15,000 feet downwind from a worst-case NO<sub>x</sub> emission. At this distance, NO<sub>2</sub> peaked at 0.3 ppm and averaged about 0.147 ppm over a short time period. The Environmental Protection Agency requires that the one-hour average concentration of NO<sub>2</sub> not exceed 0.1 ppm. It is believed that the hour-long average was much lower than 0.1 ppm at 15,000 feet. The dispersion of these two blasts indicates that moderate to severe NO<sub>x</sub> emissions are capable of dispersion to relatively safe levels over short distances. As a result, mines that are remote or of considerable scale naturally provide an efficient safeguard for the public; however, large-scale blasting near mine permit boundaries may require special consideration for uncontrolled structures or public roads that are within close proximity downwind.

Risk to the health and safety of both mine employees and the public is believed to be low, based on the preliminary sampling and observations presented in this document; however, it is prudent to quantify risk using *blast area exclusion zones*, which are an extension of

the *blast area*, as it is defined by the Mine Safety and Health Administration. Determining an exclusion zone requires a forecast of the expected intensity of the NO<sub>x</sub> emission, which can be reasonably predicted once either (1) a case history of NO<sub>x</sub> emissions is developed for an individual mine – including direct samples of gases, sleep time of explosives, estimated water exposure of the bulk agent, scale of the blast, and weather conditions – or (2) a broader body of knowledge regarding the relationship between NO<sub>x</sub> and such variables is developed. Mine employees will benefit most from the exclusion zone, due to their generally closer proximity to the blast origin.

Geometric dispersion models developed during this experiment can be used to estimate the unit volume of NO<sub>x</sub> (liters per kilogram of explosive) or predict the instantaneous peak concentration of NO<sub>2</sub> generated by a full-scale surface blast. The models are valuable because of their simplicity and their attunement to real world events. They can be constructed individually on a blast-by-blast basis and results can be validated using peer-reviewed lab data. Future studies should consider adopting the proposed geometric modelling method, or a similar technique that reduces the burden of computer modelling while preserving a reasonable mathematical interpretation of emission characteristics.

In conclusion, the direct sampling method demonstrated in this document is suitable for future research. It is capable of supplementing the current, qualitative assessment of NO<sub>x</sub> and can be used to develop blast area exclusion zones for individual mines that generate regular or substantial NO<sub>x</sub> emissions. The preliminary sampling data presented are new to the body of scientific knowledge and provide a foundation for the quantitative evaluation of blast-generated NO<sub>x</sub>. Additional measurements during diverse wind speeds and temperatures are needed to form a comprehensive health and safety conclusion; however,

the results of this study suggest that blast-generated clouds with visible concentrations of NO<sub>2</sub> are generally perceived as more dangerous than actuality. The Office of Surface Mining Reclamation and Enforcement should consider sUAS technology as a means of quantifying the toxicity and dispersion of blast-generated NO<sub>x</sub>, during its rulemaking period. Although it is understood that visible concentrations of NO<sub>2</sub> are hazardous, a broader, quantitative context is required in order to fully define risk to human health and safety in a mining environment.

## Appendix

Table A1: Flight A Weather Data

WEATHER VARIABLE	VALUE	UNITS
Temperature	62	°F
Wind Speed	13*	mph
Wind Direction	E	--
Overall Conditions	Rain	--
Atmospheric Pressure	29.78	inHG
Humidity	90%	--
Dew Point	38	°F

\*Gusts up to 25 mph

Table A2: Flight B Weather Data

WEATHER VARIABLE	VALUE	UNITS
Temperature	58	°F
Wind Speed	11	mph
Wind Direction	SE	--
Overall Conditions	P. Cloudy	--
Atmospheric Pressure	29.97	inHG
Humidity	50%	--
Dew Point	39	°F

Table A3: Flight C Weather Data

WEATHER VARIABLE	VALUE	UNITS
Temperature	53	°F
Wind Speed	8	mph
Wind Direction	SE	--
Overall Conditions	P. Cloudy	--
Atmospheric Pressure	29.92	inHG
Humidity	65%	--
Dew Point	43	°F

Table A4: Flight B Shot Details

<b>SHOT REPORT INFORMATION</b>	<b>VALUE</b>	<b>UNITS</b>
Total ANFO Weight	148,235	lbs
Total Emulsion Weight	181,997	lbs
Total Bulk Product Weight	330,232	lbs
ANFO Percentage	44.9%	--
Emulsion Percentage	55.1%	--
Total Explosives Weight	330,431.5	
Listed Blend	50/50 or 60/40	--
Ammonium Nitrate	142,306	lbs
Fuel Oil	5,929	lbs
Additives	None	--
Shot Time	10:22 AM	--
Detonator Type	Electronic	--

Table A5: Flight B Shot Design

<b>SHOT DESIGN PARAMETERS</b>	<b>VALUE</b>	<b>UNITS</b>
Burden	46	ft
Spacing	26	ft
Average Hole Depth	53	ft
Max Hole Depth	73	ft
Stemming Height	28	ft
Stemming Type	Cuttings	--
Number of Holes Loaded	267	--
Number of Holes Attempted	328	--
Volume Shot	1,031,572	BCY
Lbs per Loaded Hole	1,237.6	lbs
Lbs per 8 ms	4,503.5	lbs
Powder Factor	0.32	lbs/BCY

Note that volume is calculated as 53 feet + 18 feet (holes are held off of the coal by 18 feet).

## References

- 30 CFR § 56.2. 2004. "Definitions." Mine Safety and Health Administration (MSHA).
- 30 CFR § 77.2. 1999. "Definitions." MSHA.
- 40 CFR § 50-97. 2010. "Air Programs." Environmental Protection Agency (EPA).
- 40 CFR § 50.11. 2010. "National primary and secondary ambient air quality standards for oxides of nitrogen (with nitrogen dioxide as the indicator)." EPA.
- 95<sup>th</sup> Congress. 1977. "Surface Mining Control and Reclamation Act." Public Law 95-87.
- ACGIH (American Conference of Governmental Industrial Hygienists). 2012. "Nitrogen Dioxide." *Threshold Limit Values (TLVs) and Biological Exposure Indices (BEIs)*.
- AEISG (Australian Explosives Industry and Safety Group Inc.). 2011. "Code of Practice Prevention and Management of Blast Generated NO<sub>x</sub> Gases in Surface Blasting." 2.
- Attalla, M.I., Day, S.J., Lange, T., Lilley, W., and Morgan, S. 2008. "NO<sub>x</sub> emissions from blasting operations in open-cut coal mining." *Atmospheric Environment*. 42.34. pp. 7874-7883.
- Bajpayee, T.S., Bhatt, S.K., Rehak, T.R., Mowrey, G.L., and Ingram, D.K. 2003. "Fatal Accidents due to Flyrock and Lack of Blast Area Security and Working Practices in Mining." *Journal of mines, metals and fuels*. 51.11-12. pp. 344-349.
- Battelle. 2012. "Final Report on West Virginia Air Quality Assessment Near a Surface Coal Mine Blasting Operation." Columbus, OH.
- BLM (Bureau of Land Management). 2010. "Final Environmental Impact Statement for the Wright Area Coal Lease Applications (BLM/WY/PL-10/022+1320)." 1. U.S. Department of the Interior.
- Chaiken, R.F., Cook, E.B., and Ruhe, T.C. 1974. "Toxic fumes from explosives: ammonium nitrate-fuel oil mixtures (No. BM-RI-7867)." Bureau of Mines, Pittsburgh, Pa. Pittsburgh Mining and Safety Research Center.
- Douglas, W.W., Hepper, N.G., and Colby, T.V. 1989. "Silo-filler's disease." *Mayo Clin. Proc.* 64.3. pp. 291-304.
- Dungey, C.E. 1993. "Detailed Documentation for USAF Toxic Chemical Dispersion Model, AFTOX Version 4.1." *Environmental Protection Agency Technology Transfer Network Support Center for Regulatory Atmospheric Modeling, Alternative Air Quality Dispersion Models*.
- Eltschlager, K.K., Shuss, W., and Kovalchuk, T.E. 2001. "Carbon Monoxide Poisoning at a Surface Coal Mine, a Case Study." *Proceedings of the Annual Conference on Explosives and Blasting Technique*. International Society of Explosives Engineers (ISEE). 2.

- EPA (Environmental Protection Agency). 1980. "Compilation of Air Pollutant Emission Factors." *AP 42*. 1.5. pp 13.3-1-13.3-5.
- EPA. 2006. "Guidelines for the Reporting of Daily Air Quality – the Air Quality Index (AQI)." *EPA 454/B-06-001*. Office of Air Quality Planning and Standards. Research Triangle Park, NC.
- EPA. 2011. "Air Quality Guide for Nitrogen Dioxide." *EPA-456-11-003*. Office of Air and Radiation.
- Ermak, D.L. 1990. "User's Manual for SLAB: An Atmospheric Dispersion Model for Denser-than-air Releases (UCRL-MA-105607)." Lawrence Livermore National Laboratory.
- Frampton, M.W., Boscia, J., Roberts, N.J. Jr., Azadniv, M., Torres, A., Cox, C., Morrow, P.E., Nichols, J., Chalupa, D., Frasier, L.M., Gibb, F.R., Speers, D.M., Tsai, Y., Utell, M.J. 2002. "Nitrogen dioxide exposure: effects on airway and blood cells." *Am J Physiol Lung Cell Mol Physiol*. 282(1). pp. L155-65.
- Harris, M.L., Rowland, J.H., and Mainiero, R.J. 2004. "Blasting-related Carbon Monoxide Incident in Bristow, Virginia." *Proceedings of the Annual Conference on Explosives and Blasting Technique*. International Society of Explosives Engineers (ISEE).
- Harris, M.L., Sapko, M.J., and Mainiero, R.J. 2005. "Field Studies of CO Migration from Blasting." *Proceedings of the Annual Conference on Explosives and Blasting Technique*. International Society of Explosives Engineers (ISEE). 2.
- Helleday, R., Huberman, D., Blomberg, A., Stjernberg, N., Sandstrom, T. 1995. "Nitrogen dioxide exposure impairs the frequency of the mucociliary activity." *Eur Respir J*. 8(10). pp. 1664-8.
- Hesterberg, T.W., Bunn, W.B., McClellan, R.O., Hamade, A.K., Long, C.M., and Valberg, P.A. 2009. "Critical review of the human data on short-term nitrogen dioxide (NO<sub>2</sub>) exposures: evidence for NO<sub>2</sub> no-effect levels." *Critical reviews in toxicology*. 39.9. pp. 743-781.
- Kunkel, B.A. 1991. "AFTOX 4.0 – The Air Force Toxic Chemical Dispersion Model – A User's Guide." *PL-TR-91-2119, Environmental Research Papers No. 1083*. Phillips Laboratory, Directorate of Geophysics, Air Force Systems Command. Hanscom AFB, MA 01731-5000.
- Linaker, C.H., Coggon, D., Holgate, S.T., Clough, J., Josephs, L., Chauhan, A.J., Inskip, H.M. 2000. "Personal exposure to nitrogen dioxide and risk of airflow obstruction in asthmatic children with upper respiratory infection." *Thorax*. 55(11). pp. 930-3.
- Mainiero, R.J. 1997. "A technique for measuring toxic gases produced by blasting agents." *Proceedings of the Annual Conference on Explosives and Blasting Technique*. International Society of Explosives Engineers (ISEE). pp. 595-604.

- Mainiero, R.J., M.L. Harris, and J.H. Rowland. 1999. "Dangers of Toxic Fumes from Blasting." *Proceedings of the Annual Conference on Explosives and Blasting Technique*. 33.1. International Society of Explosives Engineers (ISEE).
- Mainiero, R.J., Rowland, J.H., Harris, M.L., and Sapko, M.J. 2006. "Behavior of Nitrogen Oxides in the Product Gases from Explosive Detonations." *Proceedings of the Annual Conference on Explosives and Blasting Technique*. International Society of Explosives Engineers (ISEE).
- NIOSH (National Institute for Occupational Safety and Health). 1979. "A Guide to the Work-Relatedness of Disease." *DHHS Publication 79-116*.
- NIOSH. 1995. "Chemical Listing and Documentation of Revised IDLH Values (as of 3/1/95)." Taft Laboratories. Cincinnati, OH.
- NIOSH. 2004. "NIOSH respirator selection logic (Publication No. 2005-100)." U.S. Department of Health and Human Services, Public Health Service, Centers for Disease Control, National Institute for Occupational Safety and Health, DHHS (NIOSH). Cincinnati, OH.
- Onederra, I., Bailey, V., Cavanough, G., and Torrance, A. 2012. "Understanding main causes of nitrogen oxide fumes in surface blasting." *Mining Technology*. 121.3. pp. 151-159.
- OSHA (Occupational Safety and Health Administration). n.d. "Table Z-1 – Limits for Air Contaminants." *29 CFR § 1910.1000*. U.S. Department of Labor.
- QG (Queensland Government). 2011. "Queensland Guidance Note QGN 20, Management of Oxides of Nitrogen in Open Cut Blasting." 3. The State of Queensland, Department of Employment, Economic Development and Innovation.
- Rowland, J., and Mainiero, R. 2000. "Factors affecting ANFO fumes production." *Proceedings of the Annual Conference on Explosives and Blasting Technique*. 1. International Society of Explosives Engineers (ISEE).
- Rowland, J., Mainiero R., and D. Hurd. 2001. "Factors affecting fumes production of an emulsion and ANFO/emulsion blends." *Proceedings of the Annual Conference on Explosives and Blasting Technique*. 2. ISEE.
- Santis, Lon D. 2001. "A Summary of Subsurface Carbon Monoxide Migration Incidents." *Proceedings of the Annual Conference on Explosives and Blasting Technique*. International Society of Explosives Engineers (ISEE). 2.
- Santis, Lon D. 2003. "An Analysis of Recent Accidents During Use of Commercial Explosives." *Proceedings of the Annual Conference on Explosives and Blasting Technique*. International Society of Explosives Engineers (ISEE).
- Sapko, M., Rowland, J., Mainiero, R., and Zlochower, I. 2002. "Chemical and Physical Factors That Influence NO<sub>x</sub> Production During Blasting-Exploratory Study." *Proceedings*

*of the Annual Conference on Explosives and Blasting Technique*. 2. International Society of Explosives Engineers (ISEE).

Schettler, L. and Brashear, S. 1996. "Effect of Water on ANFO/Emulsion Blends in Surface Mine Blasting." *Proceedings of the Twenty-Second Annual Conference on Explosives and Blasting Technique*. Orlando, FL.

Smith, D.L. 1976. "Criteria for a Recommended Standard: Occupational Exposure to Oxides of Nitrogen (Nitrogen Dioxide and Nitric Oxide)." *Washington, DC: National Institute for Occupational Safety and Health*. pp. 76-149.

Wieland, Michael S. (1998). "Understanding the Hazard Potentials of Toxic Fumes." *Eighth High Tech Seminar Blasting Technology, Instrumentation and Explosives Applications*.

WEG (WildEarth Guardians). 2014a. "Petition for Rulemaking Under the Surface Mining Control and Reclamation Act, 30 U.S.C. § 1211(g)." *OSMRE NO<sub>2</sub> Petition Body*. Office of Surface Mining Reclamation and Enforcement (OSM).

WEG. 2014b. "Petition for Rulemaking Under the Surface Mining Control and Reclamation Act, 30 U.S.C. § 1211(g)" *Exhibits*. Office of Surface Mining Reclamation and Enforcement (OSM). pp. 67-68.

## **Vita**

Robert Brendan McCray was born in Lexington, Kentucky to Robert and Brenda McCray. After his 2011 graduation from Sayre High School in Lexington, he attended the University of Kentucky (UK) and received a Bachelor of Science in Mining Engineering in 2015. During his time at UK, Brendan held three internships in the coal industry, served as a member of the University of Kentucky Explosives Research Team (UKERT), and worked as a graduate research assistant for Dr. Braden Lusk. He has been a student member of the International Society of Explosives Engineers and has co-authored one conference paper through the organization.

Robert Brendan McCray

---